

SUPEROXIDE GENERATED AT MITOCHONDRIAL COMPLEX III TRIGGERS ACUTE RESPONSES TO HYPOXIA IN THE PULMONARY CIRCULATION

Gregory B. Waypa, Jeremy D. Marks, Robert D. Guzy, Paul T. Mungai, Jacqueline M. Schriewer, Danijela Dokic, , Molly K. Ball and Paul T. Schumacker

Online Data Supplement

Additional Methods

PASMC isolation. Freshly excised rat heart and lungs were rinsed with PBS containing penicillin and streptomycin (1%). The right ventricle was cannulated, and the pulmonary vasculature was flushed with the PBS solution (30 mL). By use of the PA cannula, growth medium 199 (M199, 30 mL) containing HEPES (25 mmol/L) along with penicillin and streptomycin (1%) plus low-melting-point agarose (0.5%) and iron particles (0.5%) was flushed through the pulmonary vasculature. The iron particles were too large to pass through the capillaries; therefore, only the arteries were filled with the agarose and iron particles. The airways were filled via the trachea with M199 (15 mL) containing low-melting point agarose (1%) without iron. The lungs were placed in cold PBS to cause the agarose to gel. After 10 minutes, the lobes were dissected free and finely minced in a Petri dish. Lung fragments were resuspended and washed (3 times) with PBS by use of a magnet to retain the iron-containing fragments. The iron-containing pieces were resuspended in M199 (25 mL) containing collagenase (type IV, 80 U/mL) and incubated at 37°C for 30 to 60 minutes. To remove extravascular tissue, fragments were first drawn through a 15-gauge needle and subsequently through an 18-gauge needle. The iron containing fragments then were washed (3 times) with M199 containing FBS (20%) and drained. The resulting fragments were placed in a Petri dish containing collagen-coated (0.01%) glass cover slips and resuspended

in M199 containing FBS (10%). The Petri dishes were incubated at 37°C with CO₂ (5%) in air for 4 or 5 days, during which time the SMC were observed to migrate and adhere to the cover slips. After 4 or 5 days, the media and iron containing particles were transferred to a new dish containing fresh media. The adherent SMC continued to propagate until the cells were 50% confluent. Cells isolated by this method were confirmed to be PASMC as previously described (1E). Using a similar method, SASMC were isolated from mouse renal arteries and confirmed to be SASMC as previously described (2E). The isolated cells were cultured for 2 weeks (4 passages) and then used for the next 4 weeks (4-12 passages). In separate studies, the PA microvessels isolated by this procedure were used to determine the effects of hypoxia on the cells that comprise the pulmonary microvessels. Because the lumen of the isolated PA microvessels contain iron particles, the microvessels could be constrained in the flow-through chamber, thus allowing for their study under normoxic and hypoxic conditions.

Mouse precision-cut lung slices. Adult mice were anesthetized with ketamine (40mg/kg) and xylazine (3mg/kg). The trachea was cannulated with a 24-gauge angiocatheter. The heart and lungs were removed en bloc by using aseptic technique. The pulmonary artery was cannulated with a 1.9-Fr catheter and infused with 0.5% agarose containing Cell Tracker Red (Invitrogen, Carlsbad, CA) to label endothelial cells of the vessels. The lungs were then expanded with 1.5 ml of 1% low-melting-temperature agarose via the trachea cannula. The lungs and heart were placed in cold PBS containing 25mM HEPES to gel the agarose. By using a Leica Microsystems (Setzlar, Germany) VT 1000S tissue slicer, 200- μ m-thick lung slices were obtained and maintained in serum-free M199 media and used the same day.

Conditional Rieske iron-sulfur protein knockout mouse. The conditional RISP knockout mouse (RISP^{flox/flox}) was engineered by flanking exon 2 of the RISP gene with *loxP* sites. Implementation of the knockout was engineered by Ozgene Pty Ltd (Perth, Australia). Using homologous recombination in ES cells, *loxP* sites flanking exon 2 were introduced into the genomic locus, and chimeric mice were generated by implantation into blastocysts. Mice that underwent germ-line transmission were then bred with FLPe expressing mice to delete the PGK-neomycin selection cassette that was flanked with FRT sites. The resulting mice were then bred to homozygosity. PASMIC and SASMC isolated from these mice were cultured on glass cover slips and transduced with either an empty adenovirus (200 pfu) as a control, or Cre-expressing adenovirus (200 pfu). After 72 hours, administration of the empty or Cre-expressing adenovirus (200 pfu) was repeated. In separate studies, the PA microvessels isolated from RISP^{flox/flox} mice were transduced with either an empty adenovirus (~200 pfu) as a control, or Cre-expressing adenovirus (~200 pfu). After 72 hours, administration of the empty or Cre-expressing adenovirus (~200 pfu) was repeated. The efficacy of this regimen was confirmed using PASMIC isolated from reporter mice, *Gt(ROSA)26Sor^{tm4(ACTB-tdTomato,-EGFP)Luo}* (See Online Data Supplement Fig. 1E). The ability of the Cre-expressing adenovirus to decrease RISP expression was confirmed by Reverse Transcription PCR and Western blot (See Manuscript Fig. 2 and Online Data Supplement Fig. 7E).

Conditional smooth muscle Rieske iron-sulfur protein knockout mouse. A targeted smooth muscle conditional RISP knockout mouse was generated by crossing a SMC-heavy myosin chain-Cre expressing mouse (SMC-MHC-Cre) (3E) with a RISP^{flox/flox} mouse to generate a SMC-MHC-Cre/RISP^{flox/flox} mouse. Mice used in this study were in a mixed genetic background

(129Sv/C57BL/6). To decrease RISP expression in vascular SMC of the SMC-MHC-Cre/RISP^{flox/flox} mouse, tamoxifen (20 mg/kg body weight) dissolved in corn oil was administered i.p. for five consecutive days. Control mice received an equal volume of corn oil (Vehicle Controls). The mice were then left alone for 6 weeks to allow a sufficient time to pass in order to decrease RISP expression in the vascular SMC. The ability of tamoxifen to decrease RISP expression in the vascular SMC was confirmed by Western blot analysis of SMC isolated from the abdominal aorta (See Manuscript Fig. 7A). These mice were used for precision-cut lung slices and hemodynamic measurements.

Reverse Transcription PCR. To confirm RISP knockdown, PASMC isolated from conditional RISP knockout mice were first cultured in either the absence of adenovirus, in the presence of an empty adenovirus (at 200 pfu), or a Cre-expressing adenovirus (at 200 pfu), per the protocol described above. mRNA was then extracted from the cells using an RNeasy Mini Kit (QIAGEN Sciences, Germantown, MD) and tested by RT-PCR (30 cycles) to quantify the decrease in RISP mRNA expression. The RT-PCR product for RISP is about 600 bp, using a forward primer: 5' CTT GAA CTT GAG AAA AGG TGG GGA, and a reverse primer: 5' CCA ACT AAG TGG TTT TGC ACA GGG. β -actin was used as the internal control, using forward primer: 5' CCC AAG GCC AAC CGC GAG AAG, and reverse primer: 5' CCT CAT TGT GCT GGG TGC CAG G, which yielded a product of about 540 bp.

Western blotting. PASMC or PA vessels were washed with PBS, then lysed with buffer (Tris (50 mmol/L), NaCl (150 mmol/L), SDS (0.1%), EDTA (5 mmol/L), β -glycerophosphate (18.5 mmol/L)) containing freshly added protease inhibitor cocktail (Roche), PMSF (1 mmol/L),

sodium fluoride (10 mmol/L), and sodium orthovanadate (250 μ mol/L). Cell extracts were vortexed, incubated on ice for 20 min, centrifuged at 16,000xg for 20 min, and the supernatant was stored at -70° C. Protein extracts were electrophoresed using SDS-PAGE, and transferred to a nitrocellulose membrane. Membranes were blocked with TBS+0.1% Tween-20 (TBS-T) + 5% nonfat milk. Mouse primary antibodies against the FeS subunit (Complex III; Molecular Probes) or β -actin (Abcam) or rabbit primary antibodies against cytochrome c (Santa Cruz Biotechnology) or COX IV (Cell Signaling Technology) were added to TBS-T+5% milk+ 0.01% azide and incubated with the membrane overnight at 4° C. Membranes were washed with TBS-T, and secondary antibodies conjugated with HRP were added for 2 hr. Membranes were washed with TBS-T, stained with ECL reagent (Amersham), and exposed to film.. Multiple Westerns were quantified using ImageJ (NIH). In additional studies, the mouse abdominal aortas were dissected away from the surrounding tissue. The isolated abdominal aortas were then cut open and the inner surface was gently rubbed with a blunt instrument to remove the endothelium in order to magnify the population of vascular SMC. The abdominal aortas were washed with PBS, then lysed with buffer (Tris (50 mmol/L), NaCl (150 mmol/L), SDS (0.1%), EDTA (5 mmol/L), β -glycerophosphate (18.5 mmol/L)) containing freshly added protease inhibitor cocktail (Roche), PMSF (1 mmol/L), sodium fluoride (10 mmol/L), and sodium orthovanadate (250 μ mol/L). The abdominal aortas were sonicated 3x for 10 sec, incubated on ice for 20 min, centrifuged at 16,000xg for 20 min, and the supernatant was stored at -70° C. Protein extracts were electrophoresed using SDS-PAGE, and transferred to a nitrocellulose membrane. Membranes were blocked with TBS+0.1% Tween-20 (TBS-T) + 5% nonfat milk. Rabbit primary antibodies against the FeS subunit (ProteinTech) or β -actin (Cell Signaling) were added to TBS-T+5% milk+ 0.01% azide and incubated with the membrane overnight at 4° C. Membranes were

washed with TBS-T, and secondary antibodies conjugated with HRP were added for 2 hr. Membranes were washed with TBS-T, stained with ECL reagent (Amersham), and exposed to film. Multiple Westerns were quantified using ImageJ (NIH).

Adenoviral roGFP sensors. The targeted expression of roGFP sensors has been previously described (2E). Briefly, roGFP protein contains two engineered cysteine thiols, resulting redox-sensitive excitation maxima at 400 and 484 nm, with emission at 525 nm (roGFP2) (4E). In response to changes in thiol redox potential, roGFP exhibits reciprocal changes in intensity at the two excitation maxima (5E); its ratiometric characteristics render it insensitive to expression levels (6E-8E). Expression of roGFP was targeted to the mitochondrial matrix (Mito-roGFP) by appending a 48 bp region encoding the mitochondrial targeting sequence from cytochrome oxidase subunit IV, to the 5' end of the coding sequence. Expression of roGFP was targeted to the mitochondrial inter-membrane space (IMS-roGFP) by appending it to the carboxy terminus of glycerol phosphate dehydrogenase (GPD).

YC2.3 FRET Sensor. A genetically-encoded FRET-based sensor was used to measure $[Ca^{2+}]_i$ as previously described (9E). YC2.3 is a high affinity Ca^{2+} sensor, consisting of CFP and citrine, linked by a calmodulin-M13 hinge region (10E-12E). When bound to Ca^{2+} , FRET between CFP and citrine increases (12E). An increase in $[Ca^{2+}]_i$ is reflected by an increase in the citrine/CFP intensity ratio (535/470). YC2.3 was packaged in a recombinant adenovirus to permit efficient expression in PASMCMC.

Adenoviral infection. PASMC or SASMC on cover slips were transduced with adenoviruses to express roGFP in cytosol, IMS or mitochondrial matrix, or to express YC2.3 FRET in the cytosol. PASMC or SASMC were infected with 200 pfu per cell (Cyto-roGFP, IMS-roGFP, Mito-roGFP or YC2.3) in complete medium for 24 hrs and then changed to complete medium without virus. Experiments on the PASMC or SASMC were performed 36 to 48 hrs after infection. In separate studies, the isolated PA vessel segments (described above) that were transfected with either an Empty adenovirus or Cre Adenovirus to knock down RISP were then transduced with adenoviruses to express roGFP in cytosol or mitochondrial matrix. The PA vessels were infected with ~400,000 pfu per ml (Cyto-roGFP or Mito-roGFP) in complete medium (M199 with 10% FBS) for 24 hrs and then changed to complete medium without virus. Experiments were performed on the isolated PA vessels 36 to 48 hrs after infection with the roGFP adenovirus.

FURA-2. Hypoxia-induced changes in $[Ca^{2+}]_i$ in precision-cut lung slices were measured using FURA-2 (Invitrogen, Carlsbad, CA) as previously described (13E). Lung slices were loaded with FURA-2AM at 37°C (5 μ M) for 1 h before imaging. The lung slices were then incubated for an additional 15 min in medium without FURA-2AM to allow esterases to cleave the diacetate moiety completely. Although FURA-2AM was taken up by most cells within the lung slice, $[Ca^{2+}]_i$ measurements were restricted to regions localized to pulmonary arteries identified by Cell Tracker Red. Because a buffered salt solution was being used to perfuse the cells, endothelin 1 (ET-1; 10 nM) was added to the perfusate 15 minutes before hypoxia to prime the cells. The 15 minutes was enough time to allow for the FURA 2 ratio to return to baseline. This had the added benefit of confirming that the cells retained the ability to increase cytosolic

calcium via a receptor-mediated trigger (See Online Data Supplement Fig. 8E).

TMRM. To determine the effects of decreasing RISP expression on mitochondrial membrane potential ($\Delta\Psi_m$), additional studies were carried out using tetramethylrhodamine, methyl ester (TMRM; Invitrogen, Carlsbad, CA). This cationic dye equilibrates across the mitochondrial inner membrane in accordance with the $\Delta\Psi_m$, and changes in fluorescence at non-quenching concentrations can be used to detect changes in mitochondrial polarization. PASMC on cover slips were loaded with TMRM (0.1 nM) for 1 hour at 37°C. The cells were then placed in a flow-through chamber on an inverted microscope and perfused with BSS containing TMRM (0.1 nM). Fluorescence images were obtained under baseline conditions until a stable baseline was established. Changes in the membrane potential were assessed using the ATP-synthase inhibitor oligomycin (5 $\mu\text{g/ml}$). This was followed by the administration of carbonyl cyanide m-chloro phenyl hydrazone (CCCP; 10 μM) to dissipate the proton gradient across the inner membrane.

Time-lapse microscopy. Two days after adenoviral infection, cover slips were mounted in a sealed flow-through chamber and immediately perfused with a balanced salt solution. Under xenon illumination, cells were observed under epifluorescence using a 40x, 1.3 NA Plan Fluor objective in an inverted microscope (Nikon, Japan), and imaged with a cooled CCD camera (Photometrics, Tucson, AZ) connected to a computer workstation running Metafluor imaging software (Universal Imaging, Downingtown, PA). The roGFP was sequentially excited using 14 nm bands of light centered on 400 nm and 485 nm, while emission in a 30-nm wide band of fluorescence centered on 525 nm was imaged. Fluorescence measurements were made every 60

s before and during perfusion of hypoxic solutions. For each pair of fluorescence images, a ratiometric image (485 nm /400 nm image) was obtained. Regions of interest were created on cells, and mean fluorescence intensities and ratios were calculated for each region. Intensities and ratios were plotted on a region-by-region basis as a function of time. The YC2.3 FRET sensor was excited at 430 nm, while fluorescence emission images were obtained at 470 nm (FRET donor, CFP) and 535 (FRET acceptor, citrine) to measure changes in $[Ca^{2+}]_i$. Fura-2 was excited at 340 nm and 380 nm, while fluorescence emission images were obtained at 595 nm to measure changes in $[Ca^{2+}]_i$. The ratio of the 595 nm emission from excitation at 340 nm (bound to Ca^{2+}) to excitation at 380 nm (not bound to Ca^{2+}) were calculated and graphed. TMRM was excited at 546 nm, while fluorescence emission images were obtained at 625 nm to measure changes in $\Delta\Psi_m$. The change fluorescence emission at 625 nm, normalized to the difference in baseline fluorescence and after CCCP administration, were calculated and graphed.

Induction of hypoxia. At baseline, cells were perfused with a balanced salt solution bubbled with 21% O₂, 5% CO₂, 74% N₂ gas. Hypoxia was induced by equilibrating the solution for 1 hour with 1.5% O₂, 5% CO₂, 93.5% N₂ gas. O₂ concentration was controlled by delivering solutions to the glass-sealed chamber with flexible stainless steel tubing. Upon switching to hypoxia, the oxygen tension of the media superfusing the cells decreased from 21% O₂ to 2.5% O₂ within 3 minutes. Cells were maintained at 35.0±0.2°C.

Calibration of the roGFP response. Raw ratio values were converted to an estimate of percent oxidation on a cell-by-cell basis by obtaining ratio images of the probe at maximal reduction and maximal oxidation at the end of each experiment. Cyto-roGFP, IMS-roGFP, and

Mito-roGFP were maximally reduced with dithiothreitol (DTT; 1 mM) and maximally oxidized with *tert*-butyl hydroperoxide (tBH; 1 mM). Ratio values were calibrated to percent oxidized using the equation:

$$\%roGFP \text{ Oxidized}_T = [(roGFP_T - roGFP_{DTT}) / (roGFP_{tBH} - roGFP_{DTT})] \times 100$$

where %roGFP Oxidized_T is the percent of roGFP oxidized at time = T, roGFP_T is the roGFP ratio (400_{Ex}/484_{Ex}) at time T, roGFP_{DTT} is the roGFP ratio in response to DTT, and roGFP_{tBH} is the roGFP ratio in response to tBH.

Hemodynamics. Mice were anesthetized with avertin (240 mg/kg) injected i.p. and the trachea was cannulated with a 20 ga blunt needle. The mouse was then hooked up to a small animal respirator (Harvard) at 150 breaths/min and a tidal volume 200 μ l. A median sternotomy was performed and the pericardium was opened. Hypoxia-induced changes in the right ventricular systolic pressure (RVSP) were obtained by the insertion of a Micro Tip pressure transducer catheter (Millar) into the apex of the right ventricle. Data was continuously collected on a PC and analyzed with Chart Pro software. The experimental procedure involved performing a baseline measurement of the RSVP while the mouse was ventilated with room air. The mouse was then ventilated with a hypoxic gas mixture (5% O₂/95% N₂) for 1 min and the change in the RVSP was measured. The mouse was then switched back to room air ventilation for 2 min in order to allow it to recover, then a second baseline RVSP was measured. This was followed by a second 1 min ventilation with hypoxic gas and subsequent RSVP measurement. The two baseline RVSP measurements were averaged together as well as the two hypoxic RVSP measurements for a n=1 mouse hypoxia-induced change in RVSP.

Confocal imaging of PASMC isolated from STOCK $Gt(ROSA)26Sor^{tm4(ACTB-tdTomato,-EGFP)Luo}$ mice.

To determine the efficacy of RISP deletion by Cre-expressing adenovirus in vascular SMC from conditional RISP knockout mice, PASMC were isolated from tdTomato (mT) STOCK $Gt(ROSA)26Sor^{tm4(ACTB-tdTomato,-EGFP)Luo}$ mice (The Jackson Laboratory, Bar Harbor, ME). These reporter mice carry *loxP* sites on either side of an mT cassette and express red fluorescence in all cell types. Cre expression induces deletion of the mT cassette, activating expression of a membrane-targeted EGFP (mG) cassette located 3' to the deletion site. PASMC from those mice were seeded on cover slips and treated with an empty adenovirus (200 pfu) or Cre-expressing adenovirus (200 pfu). After 72 hours, the viral treatments were repeated. After allowing 72 hours for expression, cells were fixed in 4% formaldehyde for 20 min and washed. Confocal images were obtained using a Zeiss LSM 510 META laser scanning confocal microscope with a 40X oil immersion lens and the Zeiss LSM imaging software (Carl Zeiss MicroImaging, Thornwood, NY).

Phenotype of the SMC-MHC-Cre/RISP^{flx/flx} mouse. In order to determine any changes in the phenotype of the SMC-MHC-Cre/RISP^{flx/flx} mouse after a decrease in RISP expression in the SMC, the lungs from untreated, vehicle treated, and tamoxifen treated mice were fixed by perfusion with 4% formalin via the trachea and embedded in paraffin. The tissue blocks were sliced (5 μ m), HE stained, and changes in PA wall thickening were assessed by measuring the cross-sectional area of the PA and subtracting the cross-sectional area of the lumen and dividing that number by the cross-sectional area of the PA to determine a percentage PA wall thickness. In additional studies, the hearts of untreated, vehicle treated, and tamoxifen treated mice were dissected away from the lungs and the right ventricle (RV) was dissected from the left ventricle

(LV) and the septum (S), and each was weighed. The ratio of RV/(LVS) was calculated to determine changes, if any, in RV hypertrophy (Fulton Index) as a result on decrease SMC RISP expression. Finally, changes in cardiac function as a result of decreased SMC RISP expression were assessed by echocardiography using a GE Vivid 7 System (GE Healthcare, Milwaukee, WI) with an i13L transducer (equipped with gray scale, color, and pulsed wave Doppler capabilities). The left ventricle ejection fraction, fractional shortening and heart rate were measured to assess smooth muscle RISP deletion on cardiac function.

Statistics. Changes in PA wall thickness, Fulton Index, left ventricle ejection fraction, left ventricle fractional shortening, and heart rate were analyzed by using a two-way ANOVA. A Newman-Keuls multiple-range test was used to evaluate significant differences between groups. To control for experimental differences in the hypoxic responses, experimental studies and control experiments were always carried out on the same day. Statistical significance was set at $p < 0.05$ (14E).

Additional Figures Legend

Online Data Supplement 1E. Comparison of fluorescence in PASMC from STOCK

Gt(ROSA)26Sor^{tm4(ACTB-tdTomato,-EGFP)Luo} reporter mice in control studies (A), empty virus (200 pfu) (B) or Cre-expressing adenovirus (200 pfu) treated cells (C).

Online Data Supplement 2E. Phenotype of the SMC-MHC-Cre/RISP^{flox/flox} mouse. (A)

Inflation-fixed, H&E-stained lung slices demonstrate no pulmonary vascular remodeling following decreased RISP in SMC. “PA” denotes small pulmonary arteries. Left images denote Vehicle treated mouse lung and right image denotes tamoxifen treated mouse lung. (B) Loss of RISP in SMC does not affect vascular remodeling (% wall thickness calculated as $100 \times (\text{external area} - \text{internal area}) / \text{external area}$). Values are means \pm SEM, n= 10 pulmonary arteries/mouse, 7-9 mice per group. (C) Loss of RISP in SMC does not affect right ventricular hypertrophy as assessed by the Fulton Index (The ratio of right ventricle (RV) weight to the left ventricle (LV) and the septum (S) weight). Values are means \pm SEM, n=7-9 hearts from mice in each group. (Table D) Loss of RISP in SMC does not affect cardiac function as assessed by changes in left ventricle ejection fraction and fractional shortening as measured by echocardiography. Values are means \pm SEM, n=2-3 mice per group. (E) Loss of RISP in SMC does not affect changes in heart rate when ventilated with normoxic (room air) or hypoxic (5% O₂/95% N₂) gases. Values are means \pm SEM, n=7-9 mice per group.

Online Data Supplement Figure 3E. Hypoxia-induced contraction of a pulmonary artery in a precision-cut lung slice of a Control mouse. Image of Fura-2 fluorescence (380nm excitation)

demonstrating a decrease in the diameter of a pulmonary artery before (A) and after (B) 30 minutes of superfusion with hypoxic (1.5% O₂) media.

Online Data Supplement Figure 4E. Effect of decreased RISP expression on mitochondrial membrane potential ($\Delta\Psi_m$). Tetramethylrhodamine, methyl ester (TMRM) was used to detect changes in mitochondrial polarization. Fluorescence images of PASMC on cover slips were obtained under baseline conditions until a stable baseline was established. Changes in the membrane potential were assessed using the ATP-synthase inhibitor oligomycin (5 $\mu\text{g/ml}$). This was followed by the administration of carbonyl cyanide m-chloro phenyl hydrazone (CCCP; 10 μM) to dissipate the proton gradient across the inner membrane in No Virus treated PASMC (A; typical tracing of cells on one cover slip), Empty Virus treated PASMC (B; typical tracing of cells on one cover slip) and Cre Virus treated PASMC (C; typical tracing of cells on one cover slip). The administration of oligomycin had no effect on $\Delta\Psi_m$ for untreated and Empty Virus treated PASMC (D), however in the Cre Virus-treated PASMC there was a significant decrease in $\Delta\Psi_m$. This indicates that these cells depend on cytosolic ATP production to maintain $\Delta\Psi_m$ by powering ATP-synthase in reverse. Values are means \pm SEM, n=4 cover slips per group.

*p<0.05 compared to Baseline.

Online Data Supplement Figure 5E. Increased cytosolic calcium has no effect on Cyto-roGFP fluorescence. PASMC from an untreated mouse were seeded on glass cover slips. The PASMC on cover slips were then transfected with either an empty adenovirus or the Cyto-roGFP adenovirus. On the day of the experiment, the cells transfected with the empty adenovirus were loaded with Fura 2-AM. Both groups of cells were subjected to the same experimental

conditions. The cover slips were placed in a flow through chamber on an inverted microscope and perfused with BSS under baseline conditions for 10 minutes after which the media was switched to one containing ET-1 (25 nM) in order to increase cytosolic calcium. ET-1 increased cytosolic calcium as assessed by Fura 2 (A), however it had no effect on Cyto-roGFP fluorescence (B). This indicates that an increase in cytosolic calcium does not cause a change in the redox status of the cytosol. Values are means \pm SEM, n=3 cover slips per experiment.

*p<0.05 compared to Baseline.

Online Data Supplement Figure 6E. Hypoxia does not cause changes in NAD(P)H autofluorescence in the PA of mouse lung slices. To determine if hypoxia-induced changes in NAD(P)H autofluorescence could be tainting the Fura 2 signal (Fig. 7C), lungs slices from control mice were loaded with or without Fura 2-AM then subjected to the same experimental conditions and assessed for changes in the 340/380 fluorescence ratio. Hypoxia significantly increased the 340/380 fluorescence ratio in lung slices containing Fura 2, however there was no significant change in the 340/380 fluorescence ratio of lungs without Fura 2. This indicates that hypoxia does not cause changes in NAD(P)H autofluorescence. Values are means \pm SEM, n=4 lung slices per group. *p<0.05 compared to Baseline.

Online Data Supplement Figure 7E. Effect of Cre expression on RISP expression in PA vessels from conditional knockout mice. PA microvessels isolated from RISP^{fllox/fllox} mice were transduced with either an empty adenovirus (~200 pfu) as a control, or Cre-expressing adenovirus (~200 pfu). After 72 hours, administration of the empty or Cre-expressing adenovirus (~200 pfu) was repeated. Western blot of lysates from empty adenovirus transfected

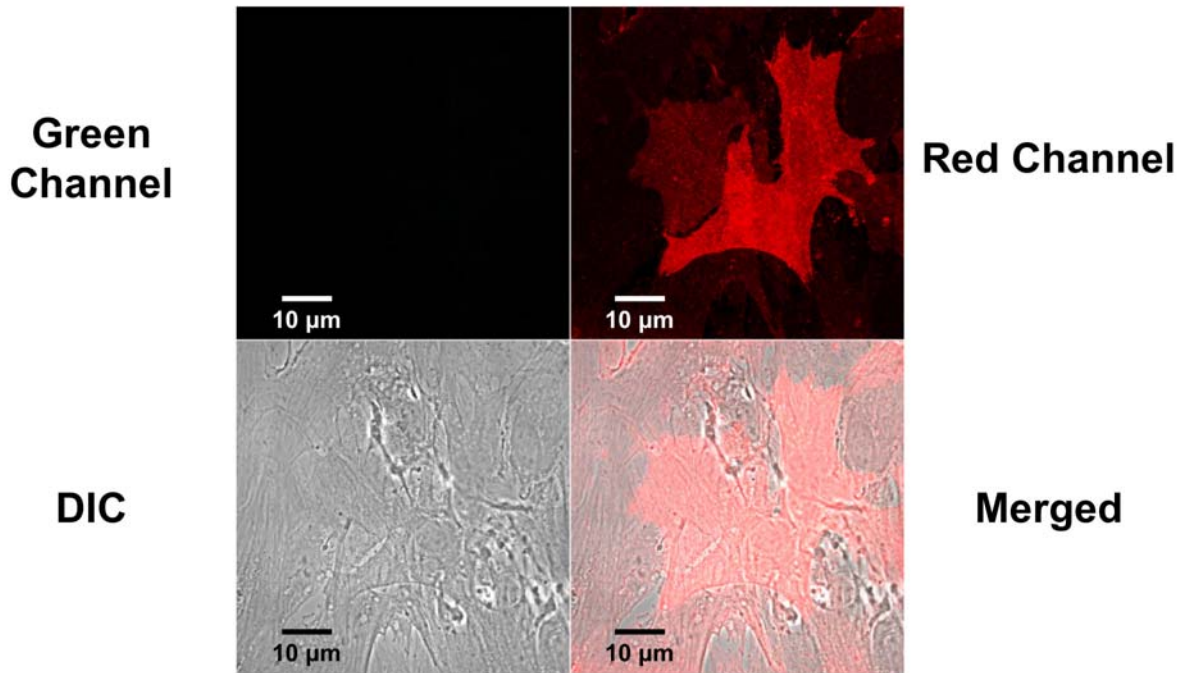
and Cre-expressing adenovirus transfected PA vessels isolated from conditional knockout mice probed with antibodies against the RISP subunit or β -actin and then quantified. Values are means \pm SEM, n=4 Westerns Blots. * $p < 0.05$ compared to empty adenovirus.

Online Data Supplement Figure 8E. Effect of decreased RISP expression on the ability of lung slices to increase cytosolic calcium, as assessed by Fura 2, in response to a receptor-mediated trigger of calcium. Lung slices from Untreated Mice (A; typical tracing of one lung slice) as well as Vehicle-treated mice and Tamoxifen-treated mice were first perfused under baseline conditions and then the media was switched to one containing ET-1 (10 nM). The average ET-1-induced change in the Fura 2 ratio was similar across the groups (B) indicating that decreased RISP expression had no effect on a receptor-mediated increase in cytosolic calcium. Values are means \pm SEM, n=6 lung slices per group.

Online Data Supplement Figure 9E. Effect of Cre expression on RISP, cytochrome c, and COX IV expression in PASMC from conditional knockout mice. (A) Western blot of lysates from untransfected (no virus), empty adenovirus-transfected (1400 pfu/cell), and Cre-expressing adenovirus-transfected (200, 600, 1000, and 1400 pfu/cell) PASMC from conditional knockout mice probed with antibodies against the RISP subunit, cytochrome c, COX IV or β -actin. (B) Quantified analysis of Western blots with RISP expression normalized to β -actin. (C) Quantified analysis of Western blots with cytochrome c expression normalized to β -actin. (D) Quantified analysis of Western blots with COX IV expression normalized to β -actin. Values are means \pm SEM, n=5 Westerns Blots. * $p < 0.05$ compared to no virus.

Online Data Supplement Figure 10E. Decreased RISP expression does not affect the ability of Cyto-roGFP to respond to the administration of exogenous hydrogen peroxide. To determine whether RISP depletion affects the ability to oxidize the Cyto-roGFP under normoxic conditions, control (No Virus), Empty Adenovirus and Cre Adenovirus-transfected PASMC were perfused with BSS under normoxic baseline conditions and then switched to BSS containing H₂O₂ (30 μM). H₂O₂ significantly increased oxidation of Cyto-roGFP to a similar extent in all groups. This indicates that the decreased RISP expression in the Cre Adenovirus-transfected PASMC does not maximally oxidize Cyto-roGFP and therefore mask the hypoxic response. Values are means ± SEM, n=4 cover slips per experiment. *p<0.05 compared to Baseline.

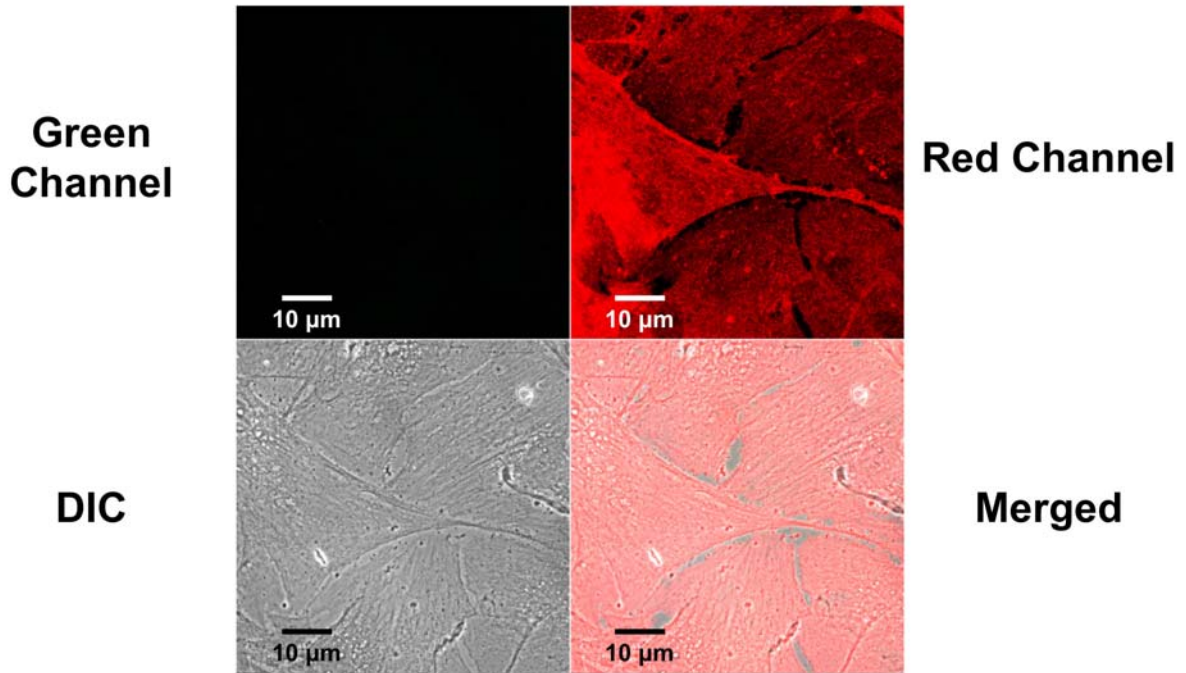
Online Data Supplement Figure 11E. Effect of decreased RISP expression on the ability of lung slices to increase cytosolic calcium, as assessed by YC2.3 FRET, in response to a receptor-mediated trigger of calcium. PASMC isolated from a RISP^{flox/flox} mouse were treated with no virus (No Adenovirus), Empty Adenovirus, or Cre Adenovirus. (A) Typical tracing of Empty Adenovirus-transfected PASMC that were perfused under baseline conditions and then switched to media containing ET-1 (25 nM). The average ET-1-induced change in the YC2.3 FRET ratio was similar across the groups (B) indicating that adenoviral-treatment of PASMC has no effect on a receptor-mediated increase in cytosolic calcium. Values are means ± SEM, n=4 cover slips with 2-3 PASMC per cover slip.



No Virus (Control)

Online Data Supplement Figure 1E (A)

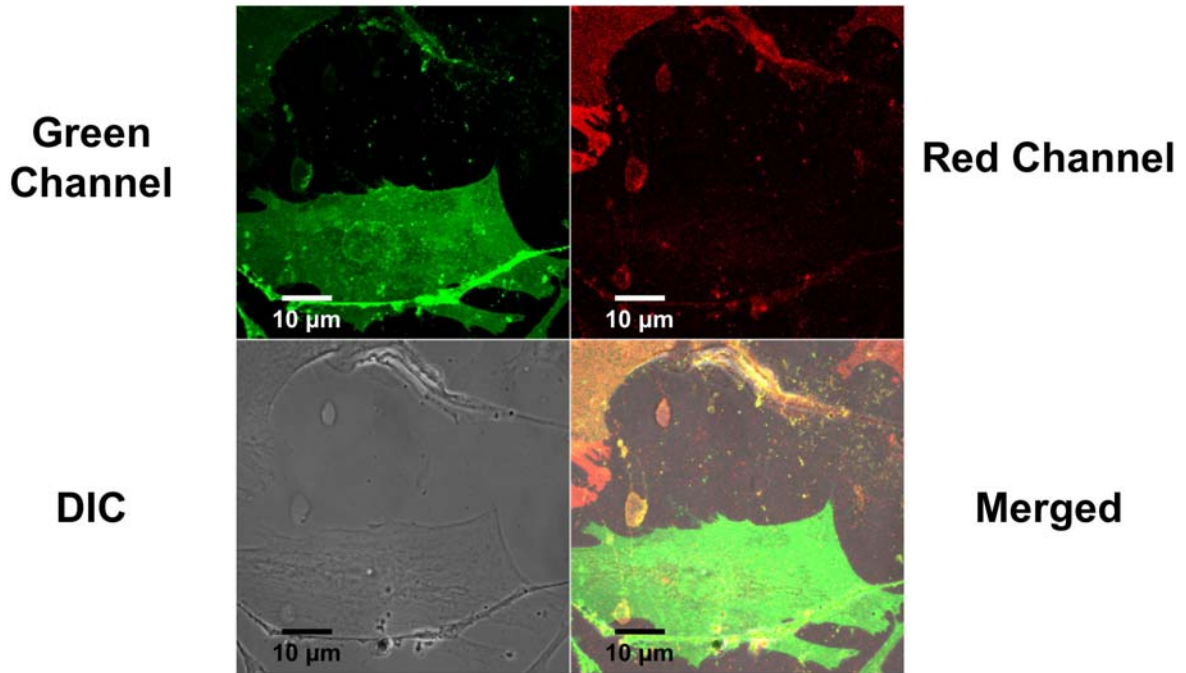
Online Data Supplement Figure 1E (A) Transfection regimen for our Cre-expressing adenovirus is sufficient for deleting a membrane-targeted tdTomato (mT) cassette from STOCK *Gt(ROSA)26Sor^{tm4(ACTB-tdTomato,-EGFP)Luo}* mice. Confocal images of PSMC isolated from STOCK *Gt(ROSA)26Sor^{tm4(ACTB-tdTomato,-EGFP)Luo}* mice left untreated (no virus).



Empty Adenovirus

Online Data Supplement Figure 1E (B)

Online Data Supplement Figure 1E (B) Transfection regimen for our Cre-expressing adenovirus is sufficient for deleting a membrane-targeted tdTomato (mT) cassette from STOCK *Gt(ROSA)26Sor^{tm4(ACTB-tdTomato,-EGFP)Luo}* mice. Confocal images of PSMC isolated from STOCK *Gt(ROSA)26Sor^{tm4(ACTB-tdTomato,-EGFP)Luo}* mice transfected with an empty adenovirus (200 pfu) for 72 hours followed by a second administration of the empty adenovirus (200 pfu) for an additional 72 hours.



Cre Adenovirus

Online Data Supplement Figure 1E (C)

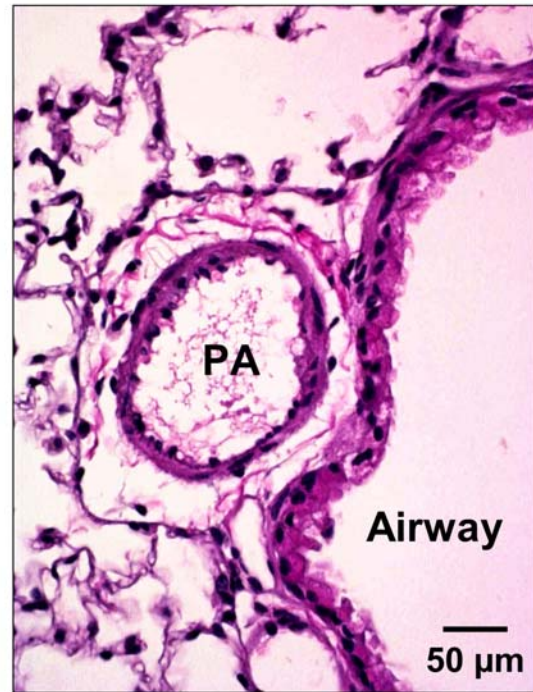
Online Data Supplement Figure 1E (C) Transfection regimen for our Cre-expressing adenovirus is sufficient for deleting a membrane-targeted tdTomato (mT) cassette from STOCK *Gt(ROSA)26Sor^{tm4(ACTB-tdTomato,-EGFP)Luo}* mice. Confocal images of PASM isolated from STOCK *Gt(ROSA)26Sor^{tm4(ACTB-tdTomato,-EGFP)Luo}* mice transfected with a Cre-expressing adenovirus (200 pfu) for 72 hours followed by a second administration of the Cre-expressing adenovirus (200 pfu) for an additional 72 hours.

SMC-MHC-Cre/RISP IoxP/IoxP



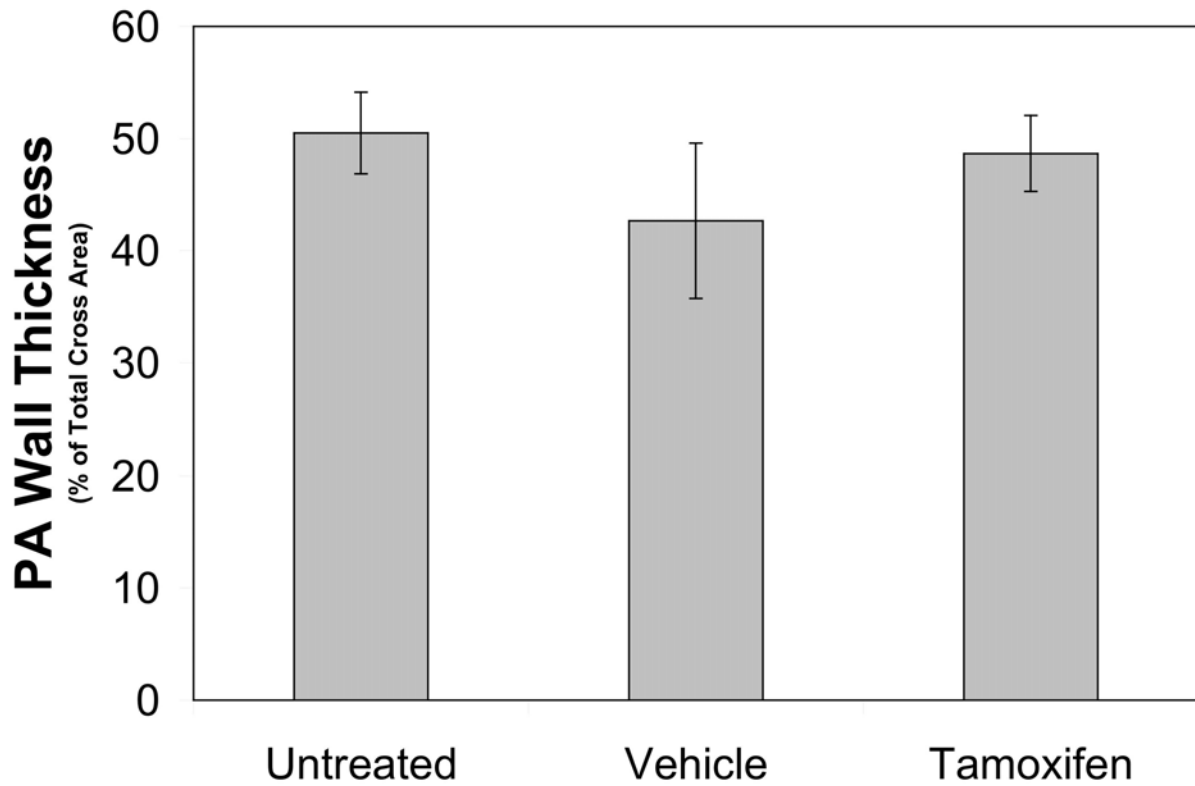
Vehicle

Online Data Supplement Figure 2E (A)



Tamoxifen

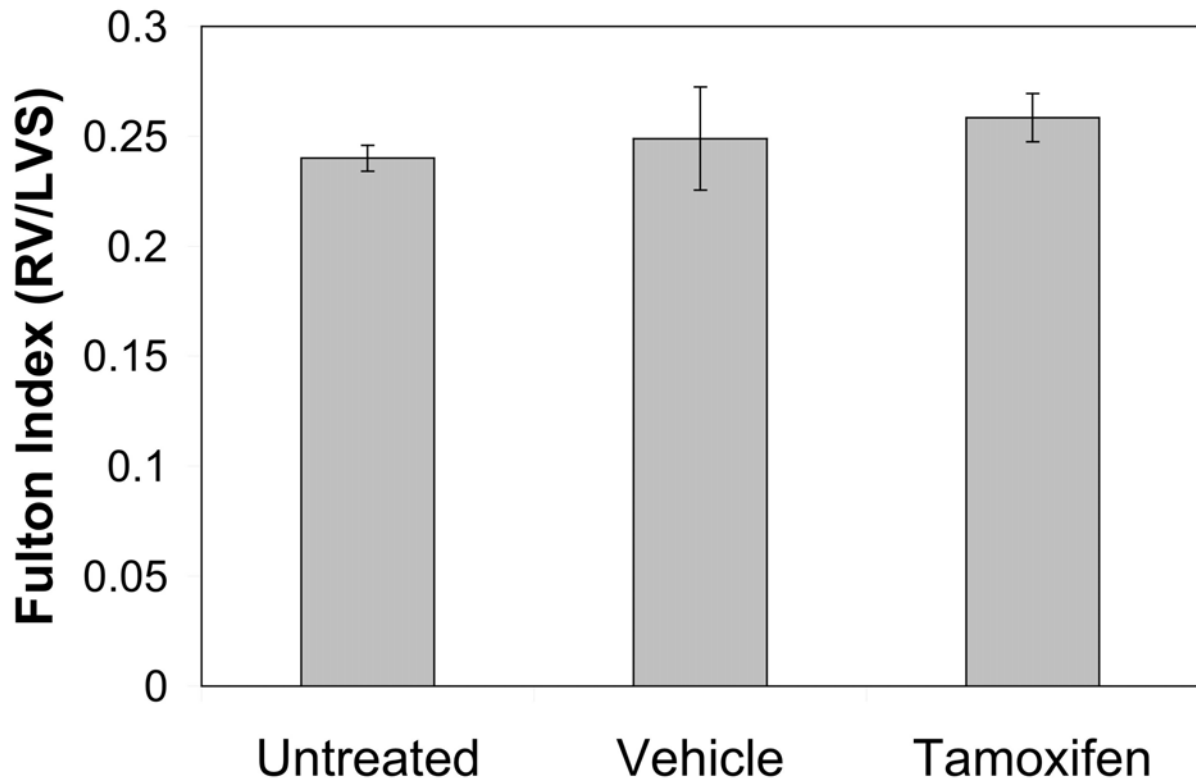
Online Data Supplement Figure 2E (A) Inflation-fixed, H&E-stained lung slices demonstrate no pulmonary vascular remodeling following decreased RISP in SMC. “PA” denotes small pulmonary arteries. Left images denote Vehicle treated mouse lung and right image denotes tamoxifen treated mouse lung.



Online Data Supplement Figure 2E (B)

Online Data Supplement Figure 2E (B) Loss of RISP in SMC does not affect vascular remodeling (% wall thickness calculated as $100 \times (\text{external area} - \text{internal area}) / \text{external area}$).

Values are means \pm SEM, n= 10 pulmonary arteries/mouse, 7-9 mice per group.



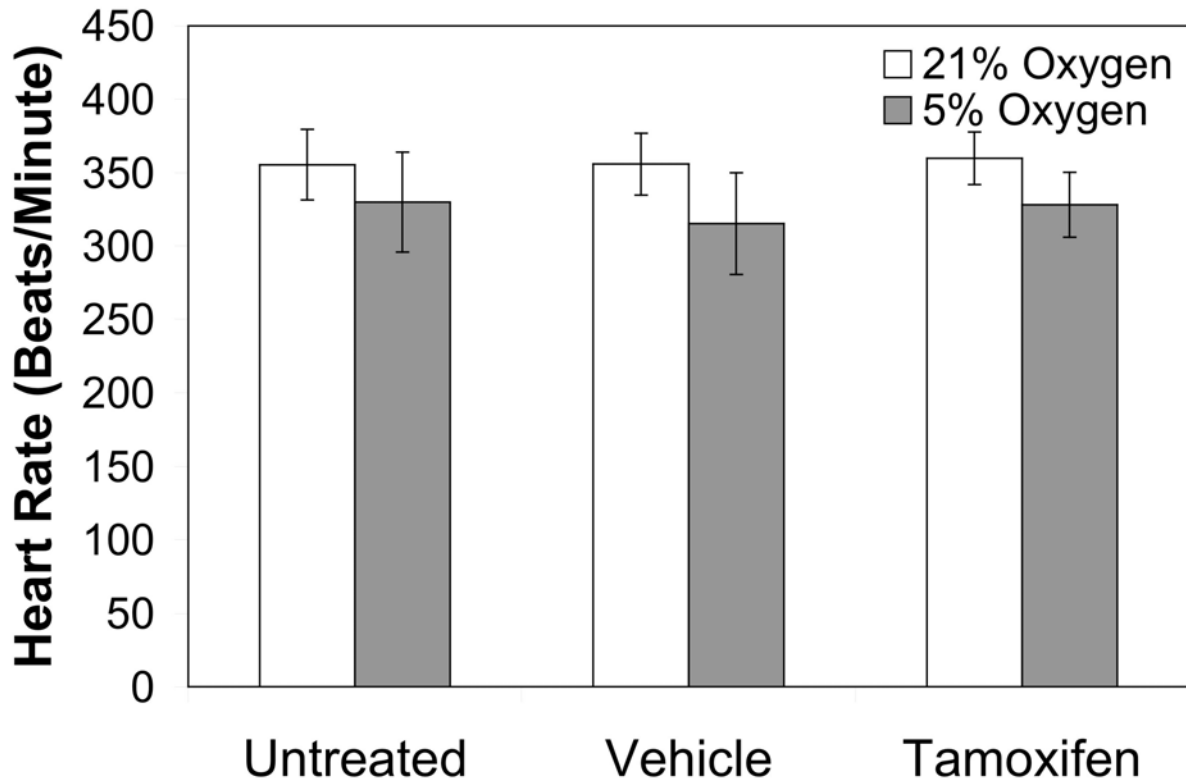
Online Data Supplement Figure 2E (C)

Online Data Supplement Figure 2E (C) Loss of RISP in SMC does not affect right ventricular hypertrophy as assessed by the Fulton Index (The ratio of right ventricle (RV) weight to the left ventricle (LV) and the septum (S) weight). Values are means \pm SEM, n=7-9 hearts from mice in each group.

Table 2E (D): Cardiac Function

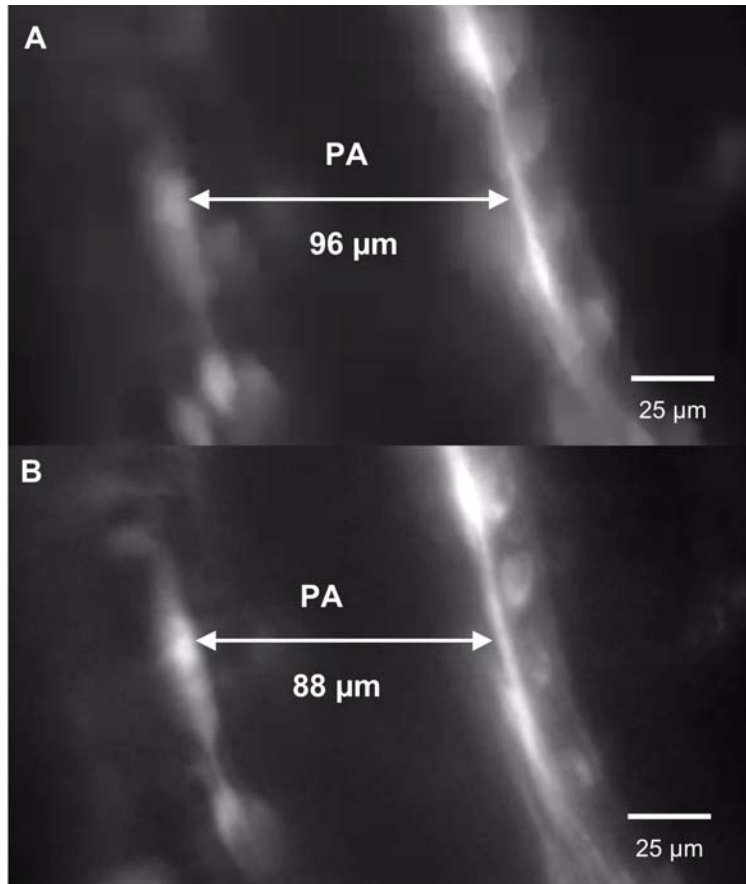
Left Ventricle	Vehicle Control	Tamoxifen
Ejection Fraction	83 ± 0.0%	84.75 ± 4.57%
Fractional Shortening	46 ± 0.0%	48.25 ± 4.99%

Online Data Supplement Table 2E (D) Loss of RISP in SMC does not affect cardiac function as assessed by changes in left ventricle ejection fraction and fractional shortening as measured by echocardiography. Values are means ± SEM, n=2-3 mice per group.



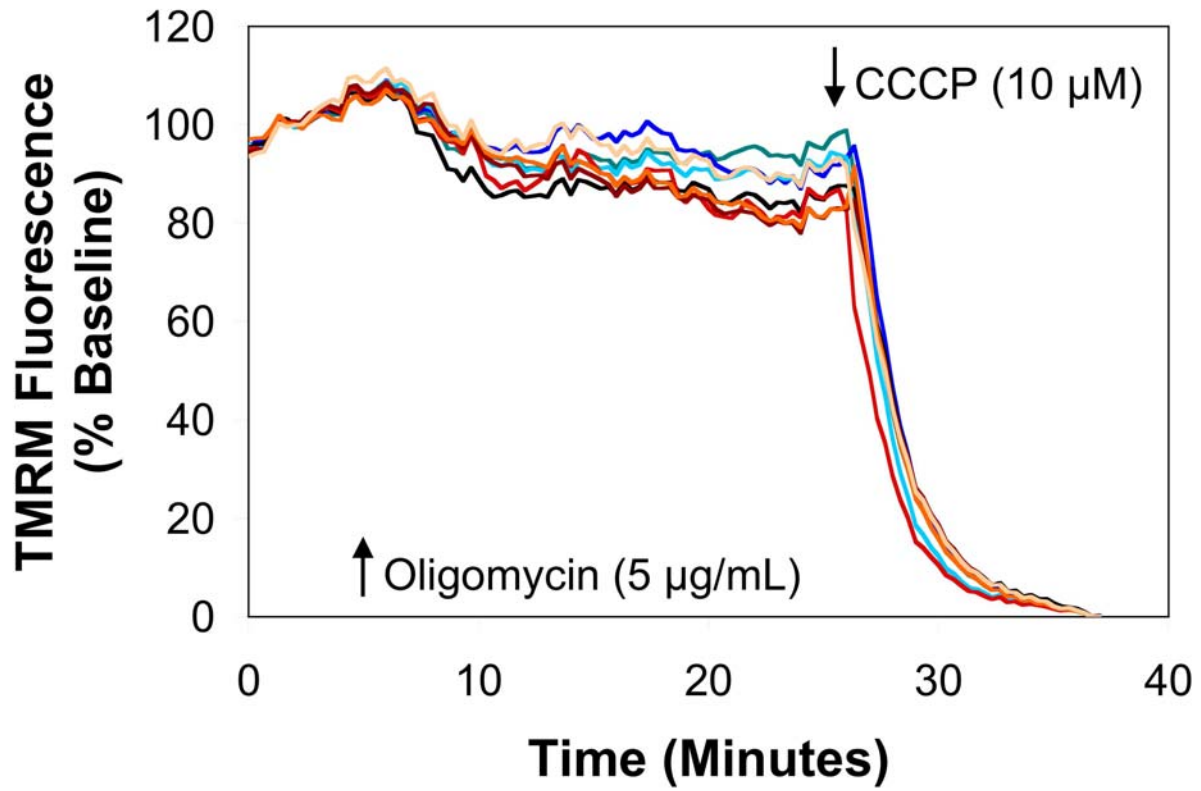
Online Data Supplement Figure 2E (E)

Online Data Supplement Figure 2E (E) Loss of RISP in SMC does not affect changes in heart rate when ventilated with normoxic (room air) or hypoxic (5% O₂/95% N₂) gases. Values are means \pm SEM, n=7-9 mice per group.



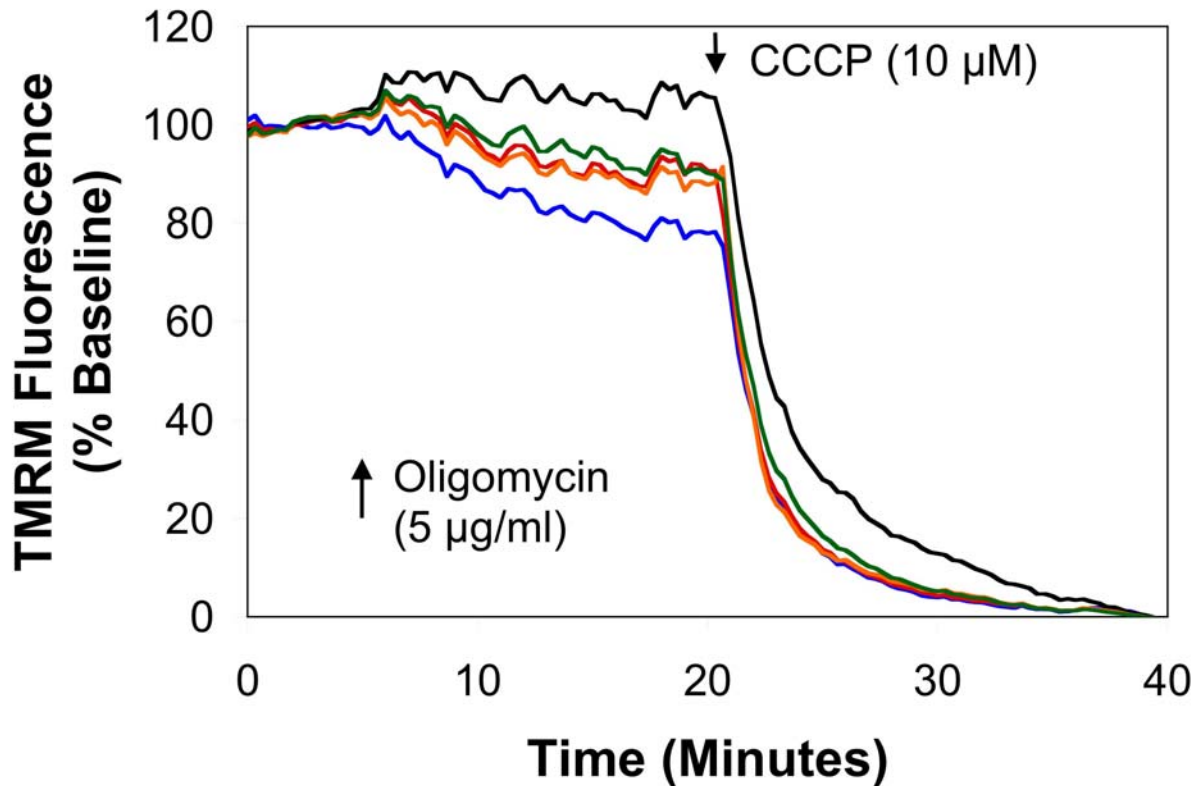
Online Data Supplement Figure 3E

Online Data Supplement Figure 3E. Hypoxia-induced contraction of a pulmonary artery in a precision-cut lung slice of a Control mouse. Image of Fura 2 fluorescence (380nm excitation) demonstrating a decrease in the diameter of a pulmonary artery before (A) and after (B) 30 minutes of superfusion with hypoxic (1.5% O₂) media.



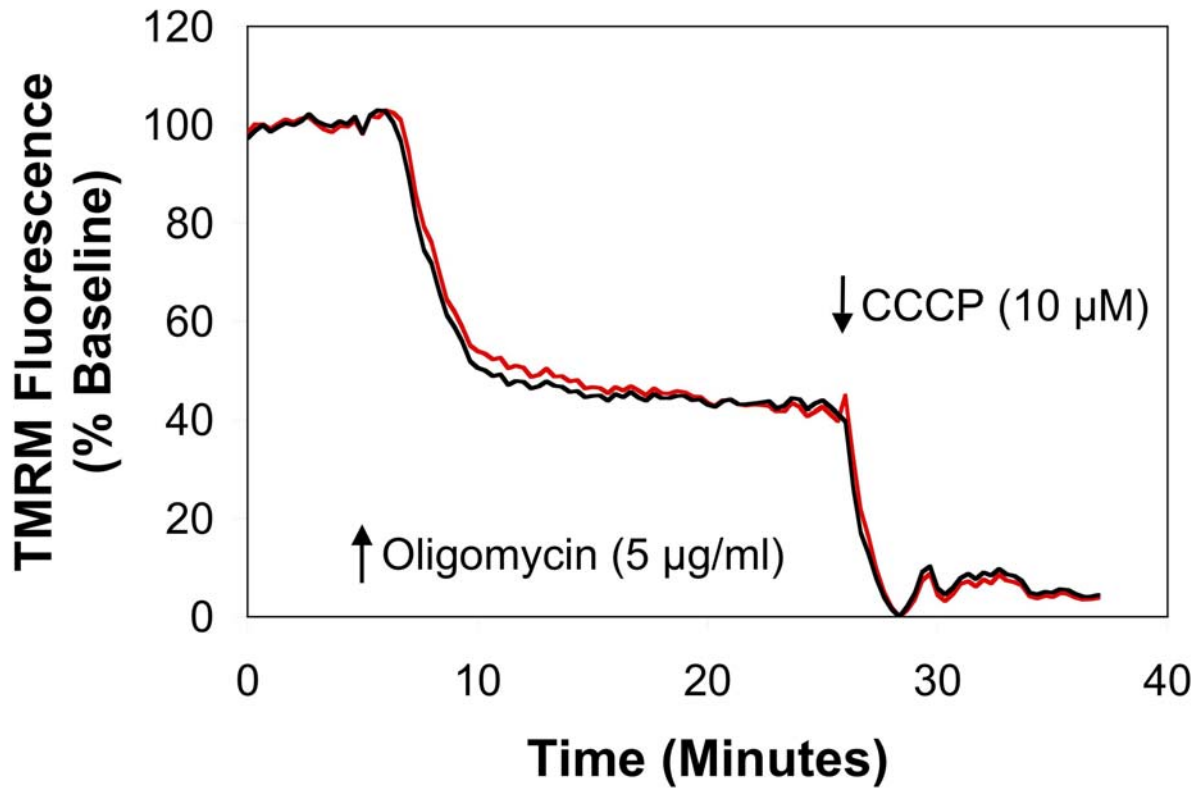
Online Data Supplement Figure 4E (A)

Online Data Supplement Figure 4E (A). Effect of decreased RISP expression on mitochondrial membrane potential ($\Delta\Psi_m$). Tetramethylrhodamine, methyl ester (TMRM) was used to detect changes in mitochondrial polarization. Fluorescence images of PASMC on cover slips were obtained under baseline conditions until a stable baseline was established. Changes in the membrane potential in response to the ATP-synthase inhibitor oligomycin (5 µg/ml) were then assessed. This was followed by the administration of carbonyl cyanide m-chloro phenyl hydrazone (CCCP; 10 µM) to dissipate the proton gradient across the inner membrane in No Virus treated PASMC (typical tracing).



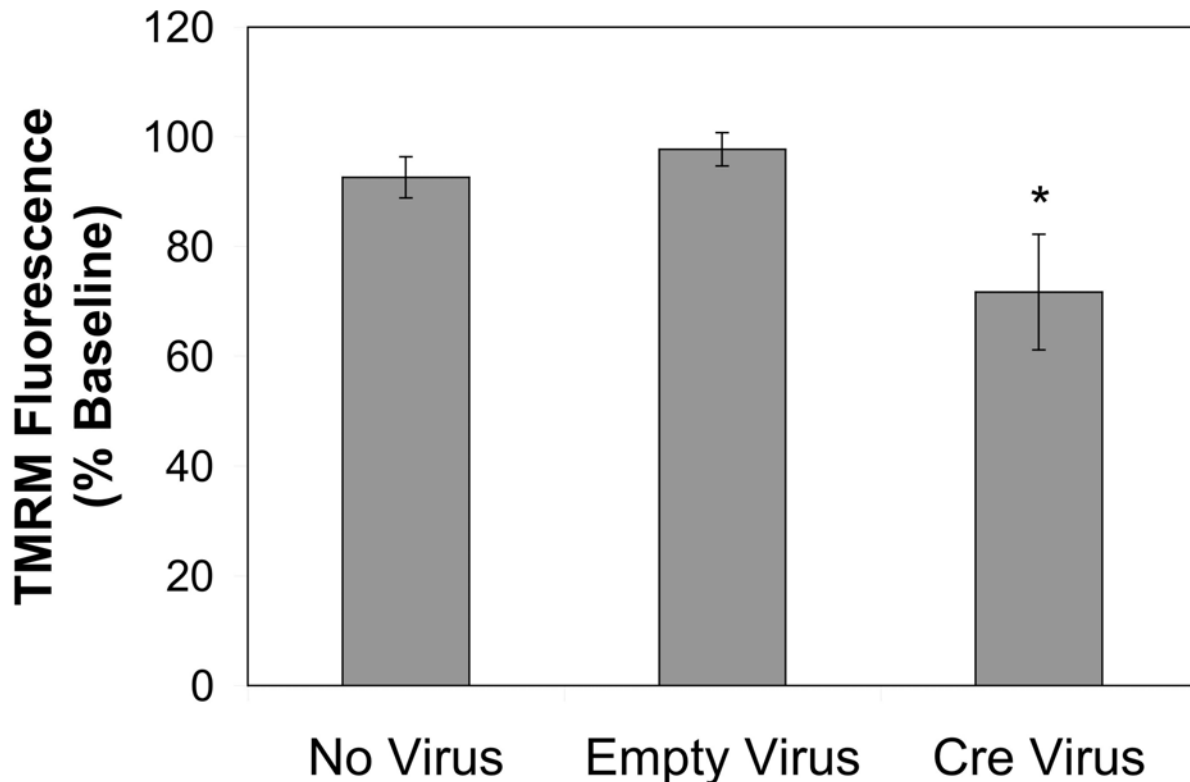
Online Data Supplement Figure 4E (B)

Online Data Supplement Figure 4E (B). Effect of decreased RISP expression on mitochondrial membrane potential ($\Delta\Psi_m$). Tetramethylrhodamine, methyl ester (TMRM) was used to detect changes in mitochondrial polarization. Fluorescence images of PASM cells on cover slips were obtained under baseline conditions until a stable baseline was established. Changes in the membrane potential in response to the ATP-synthase inhibitor oligomycin (5 µg/ml) were then assessed. This was followed by the administration of carbonyl cyanide m-chloro phenyl hydrazone (CCCP; 10 µM) to dissipate the proton gradient across the inner membrane in Empty Virus treated PASM cells (typical tracing).



Online Data Supplement Figure 4E (C)

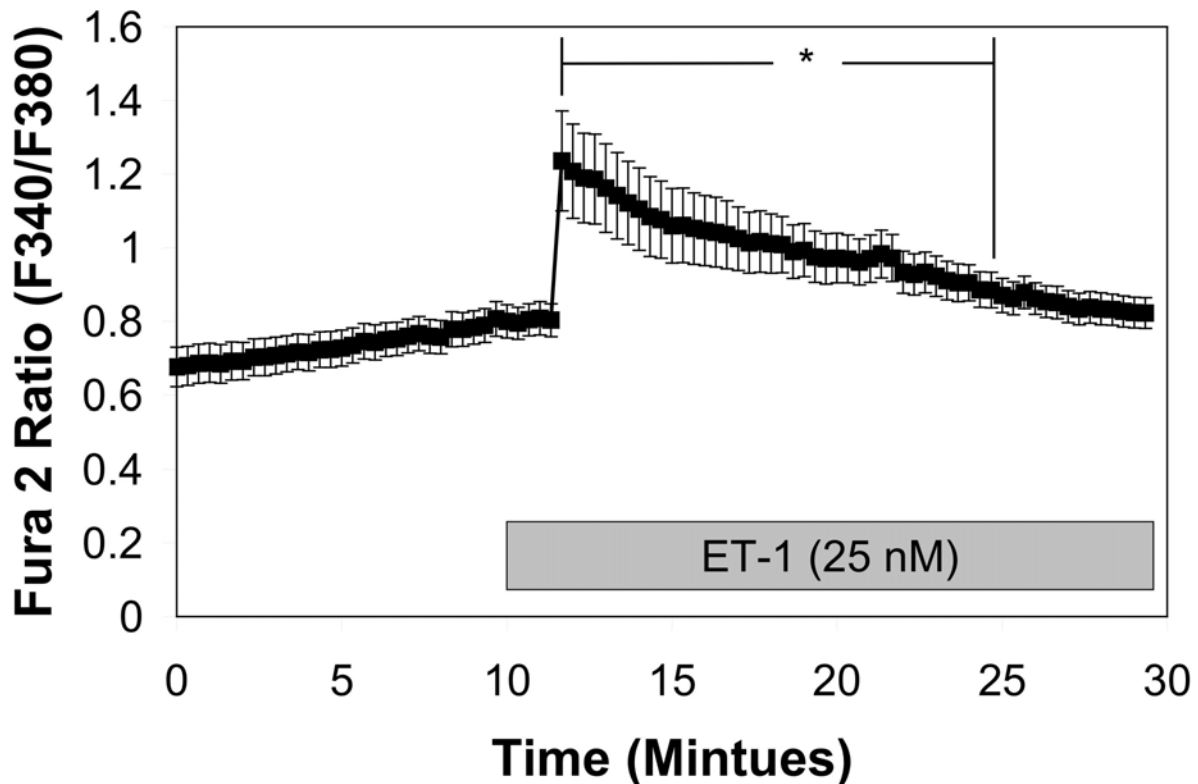
Online Data Supplement Figure 4E (C). Effect of decreased RISP expression on mitochondrial membrane potential ($\Delta\Psi_m$). Tetramethylrhodamine, methyl ester (TMRM) was used to detect changes in mitochondrial polarization. Fluorescence images of PASMC on cover slips were obtained under baseline conditions until a stable baseline was established. Changes in the membrane potential in response to the ATP-synthase inhibitor oligomycin (5 $\mu\text{g/ml}$) were then assessed. This was followed by the administration of carbonyl cyanide m-chloro phenyl hydrazone (CCCP; 10 μM) to dissipate the proton gradient across the inner membrane in Cre Virus treated PASMC (typical tracing).



Online Data Supplement Figure 4E (D)

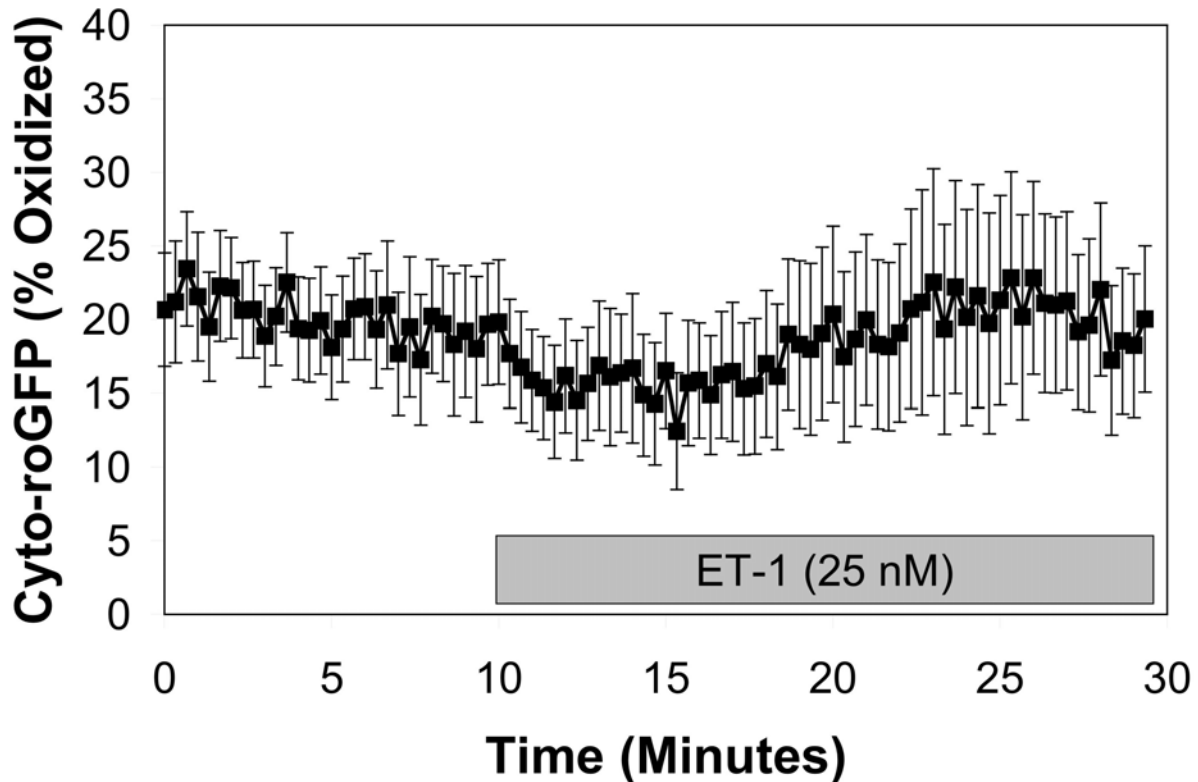
Online Data Supplement Figure 4E (D). Effect of decreased RISP expression on mitochondrial membrane potential ($\Delta\Psi_m$). Tetramethylrhodamine, methyl ester (TMRM) was used to detect changes in mitochondrial polarization. Fluorescence images of PASMC on cover slips were obtained under baseline conditions until a stable baseline was established. Changes in the membrane potential in response to the ATP-synthase inhibitor oligomycin (5 $\mu\text{g}/\text{ml}$) were then assessed. This was followed by the administration of carbonyl cyanide m-chloro phenyl hydrazone (CCCP; 10 μM) to dissipate the proton gradient across the inner membrane. The administration of oligomycin had no effect on $\Delta\Psi_m$ for untreated and Empty Virus treated PASMC (D), however in the Cre Virus-treated PASMC there was a significant decrease in $\Delta\Psi_m$. This indicates that these cells utilize glycolysis to generate ATP, and that $\Delta\Psi_m$ is maintained by

the mitochondrial importation of cytosolic ATP-to power the ATP-synthase in reverse. Values are means \pm SEM, n=4 cover slips per group. *p<0.05 compared to Baseline.



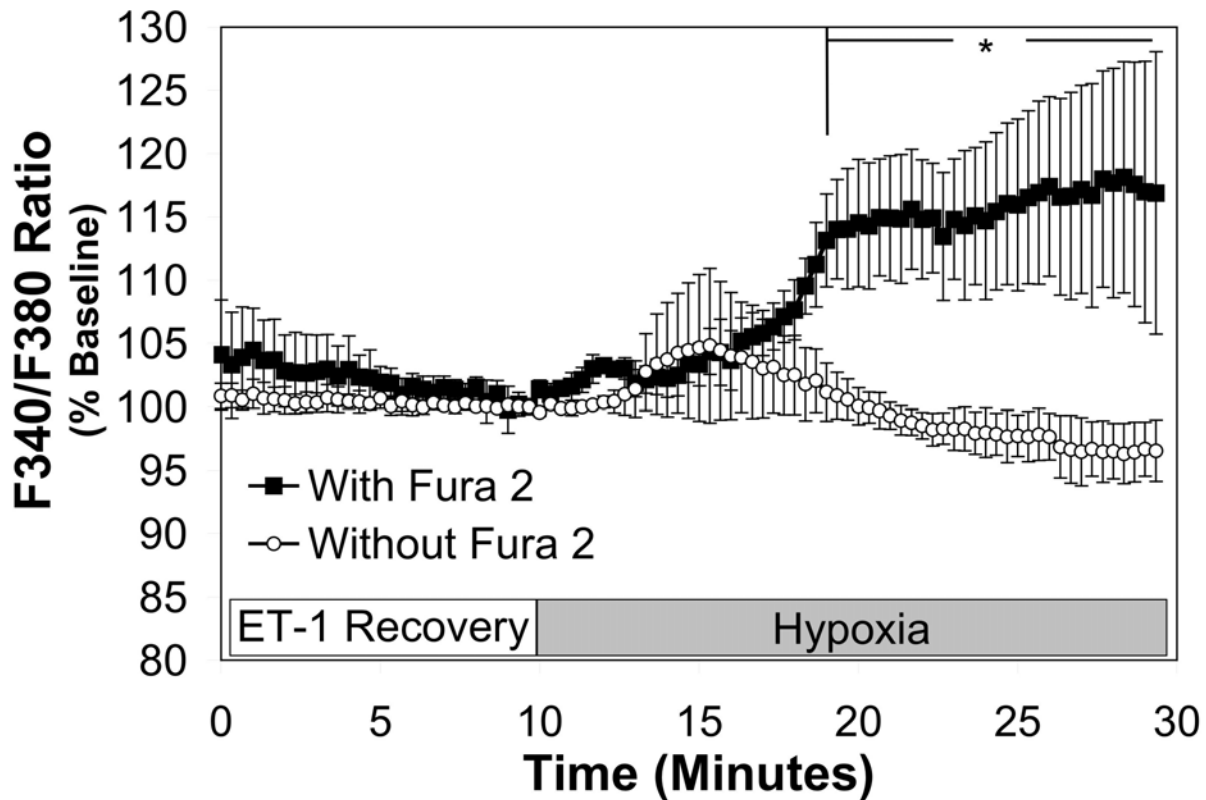
Online Data Supplement Figure 5E (A)

Online Data Supplement Figure 5E. Increased cytosolic calcium has no effect on Cyto-roGFP fluorescence. PASMCM from an untreated mouse were seeded on glass cover slips and then transfected with either an empty adenovirus or the Cyto-roGFP adenovirus. Both groups of cells were subjected to the same experimental conditions. The cover slips were placed in a flow through chamber on an inverted microscope and perfused with BSS under baseline conditions for 10 minutes after which the media was switched to one containing ET-1 (25 nM) in order to increase cytosolic calcium. (A) On the day of the experiment, cells transfected with the empty adenovirus were loaded with Fura 2-AM. ET-1 increased cytosolic calcium as assessed by Fura 2. Values are means \pm SEM, n=3 cover slips. *p<0.05 compared to Baseline.



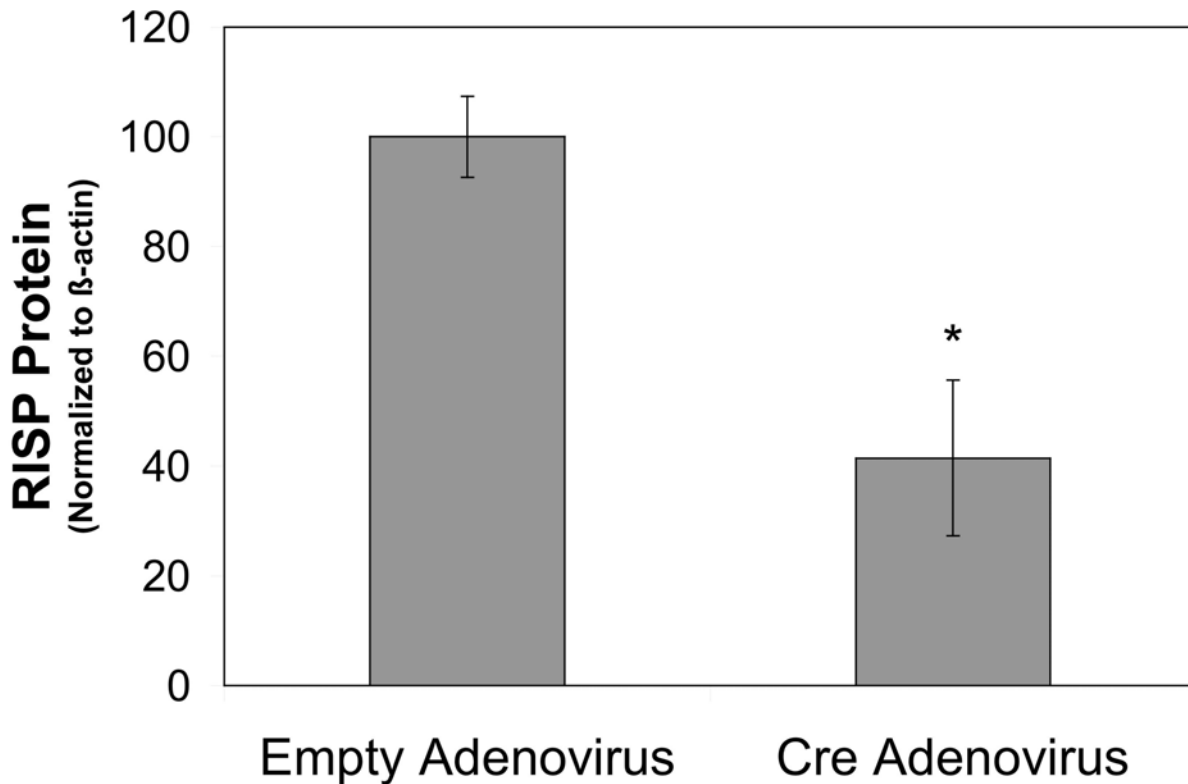
Online Data Supplement Figure 5E (B)

Online Data Supplement Figure 5E. Increased cytosolic calcium has no effect on Cyto-roGFP fluorescence. PASMIC from an untreated mouse were seeded on glass cover slips. The PASMIC on cover slips were then transfected with either an empty adenovirus or the Cyto-roGFP adenovirus. Both groups of cells were subjected to the same experimental conditions. The cover slips were placed in a flow through chamber on an inverted microscope and perfused with BSS under baseline conditions for 10 minutes after which the media was switched to one containing ET-1 (25 nM) in order to increase cytosolic calcium. **(B)** ET-1 had no effect on Cyto-roGFP fluorescence. This indicates that an increase in cytosolic calcium does not cause a change in the redox status of the cytosol. Values are means \pm SEM, n=3 cover slips.



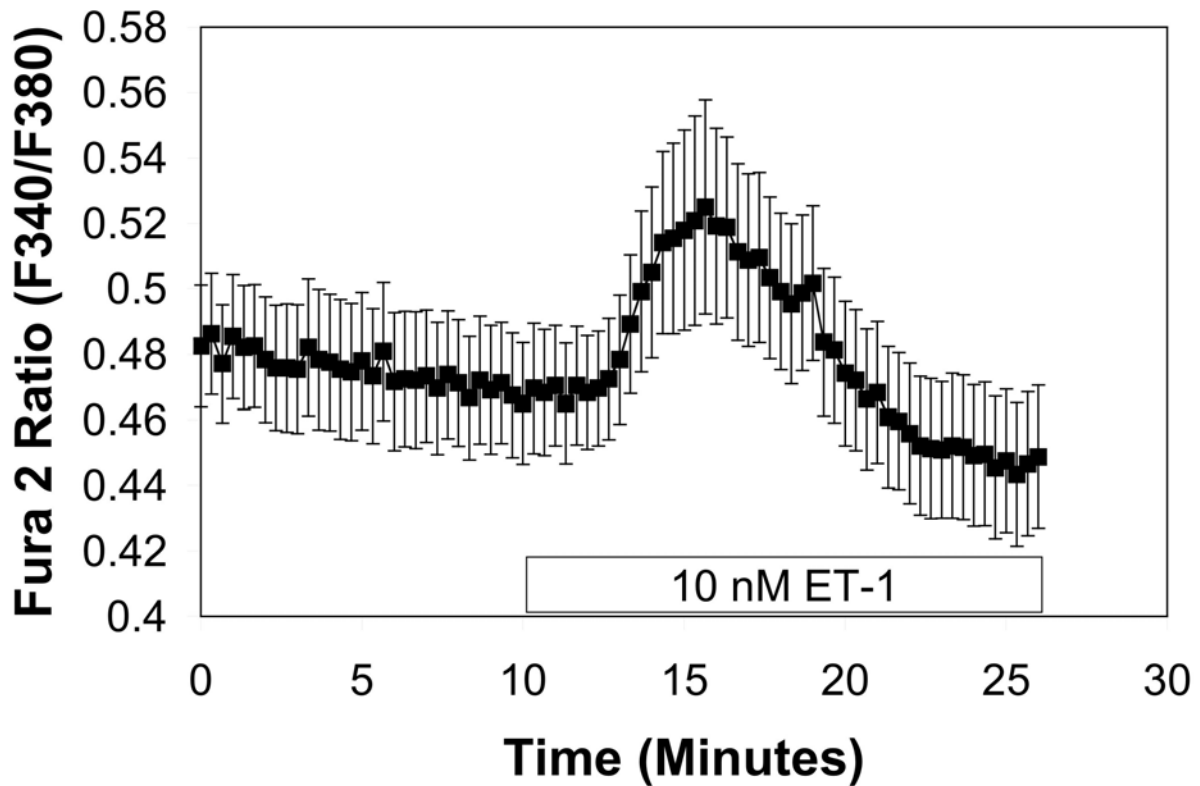
Online Data Supplement Figure 6E

Online Data Supplement Figure 6E. Hypoxia does not cause changes in NAD(P)H autofluorescence in the PA of mouse lung slices. To determine if hypoxia-induced changes in NAD(P)H autofluorescence could be tainting the Fura 2 signal (Fig. 7C), lungs slices from control mice were loaded with or without Fura 2-AM then subjected to the same experimental conditions and assessed for changes in the 340/380 fluorescence ratio. Hypoxia significantly increased the 340/380 fluorescence ratio in lung slices containing Fura 2, however there was no significant change in the 340/380 fluorescence ratio of lungs without Fura 2. This indicates that hypoxia does not alter NAD(P)H autofluorescence. Values are means \pm SEM, n=4 lung slices per group. *p<0.05 compared to Baseline.



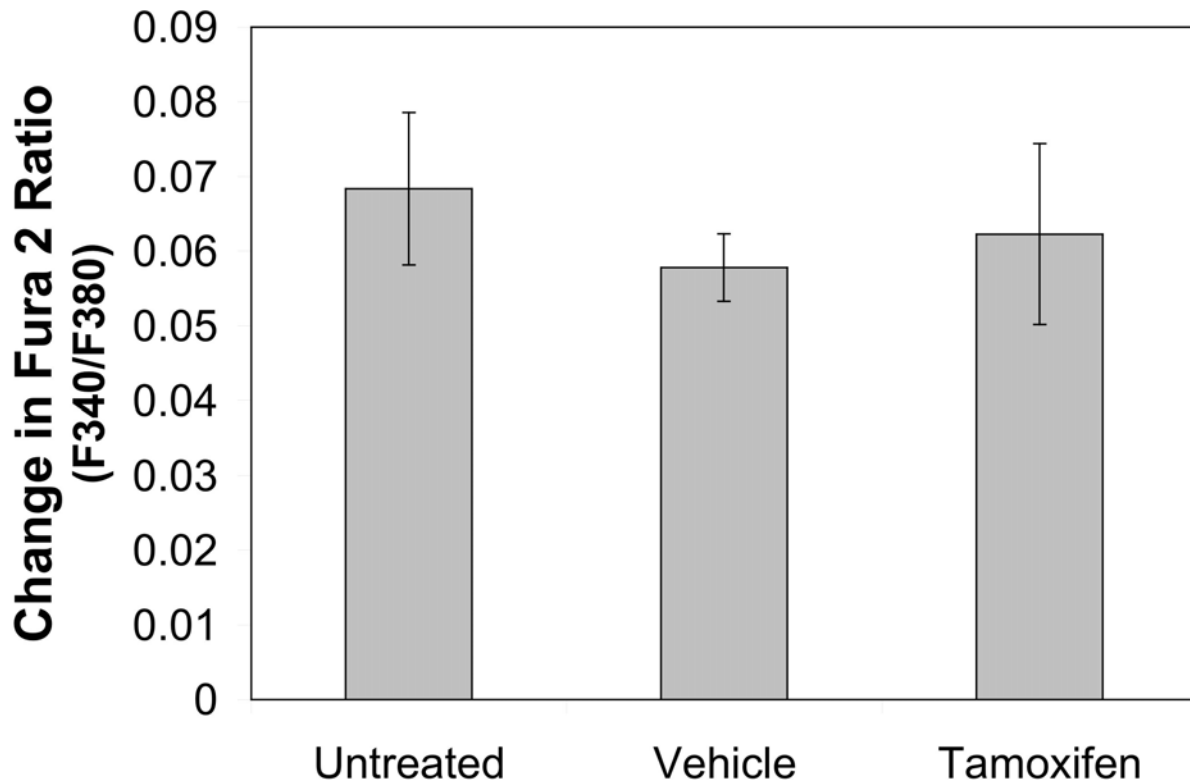
Online Data Supplement Figure 7E

Online Data Supplement Figure 7E. Effect of Cre expression on RISP expression in PA vessels from conditional knockout mice. PA microvessels isolated from $RISP^{flx/flx}$ mice were transduced with either an empty adenovirus (~200 pfu) as a control, or Cre-expressing adenovirus (~200 pfu). After 72 hours, administration of the empty or Cre-expressing adenovirus (~200 pfu) was repeated. Western blot of lysates from empty adenovirus-transfected and Cre-expressing adenovirus-transfected PA vessels from conditional knockout mice probed with antibodies against the RISP subunit or β -actin and then quantified. Values are means \pm SEM, n=4 Westerns Blots. * $p < 0.05$ compared to empty adenovirus.



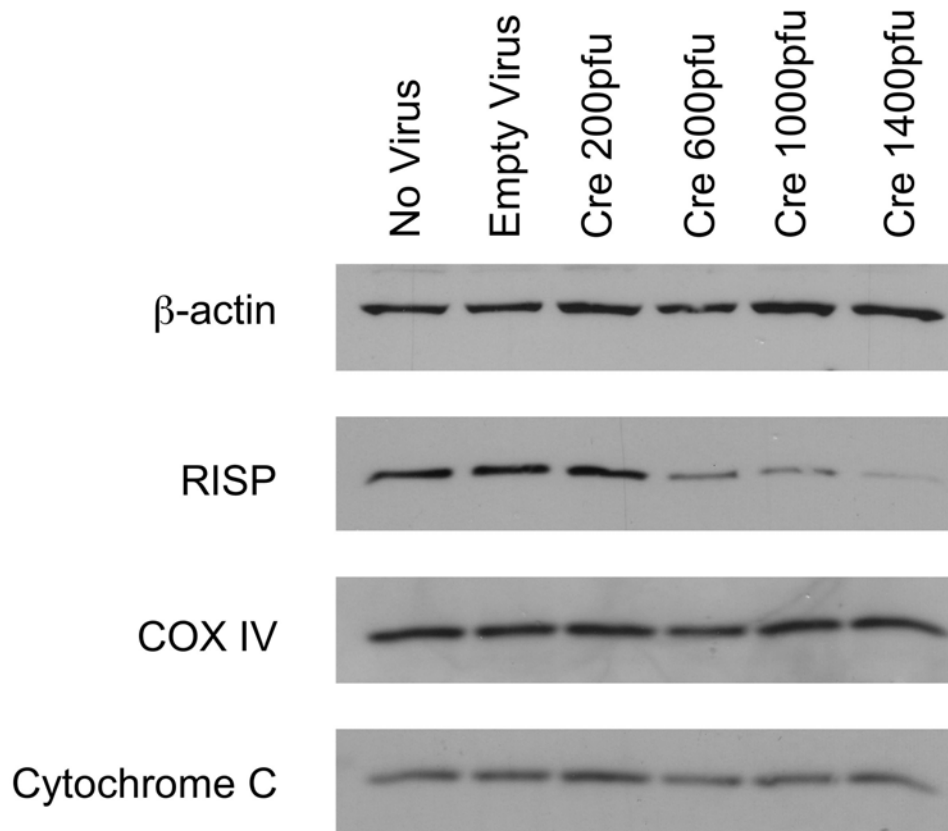
Online Data Supplement Figure 8E (A)

Online Data Supplement Figure 8E (A). Effect of decreased RISP expression on the ability of lung slices to increase cytosolic calcium, as assessed by Fura 2, in response to a receptor-mediated trigger of calcium. Lung slices from Untreated Mice (typical tracing of one lung slice) as well as Vehicle-treated mice and Tamoxifen-treated mice were perfused under baseline conditions and then the media was switched to one containing ET-1 (10 nM).



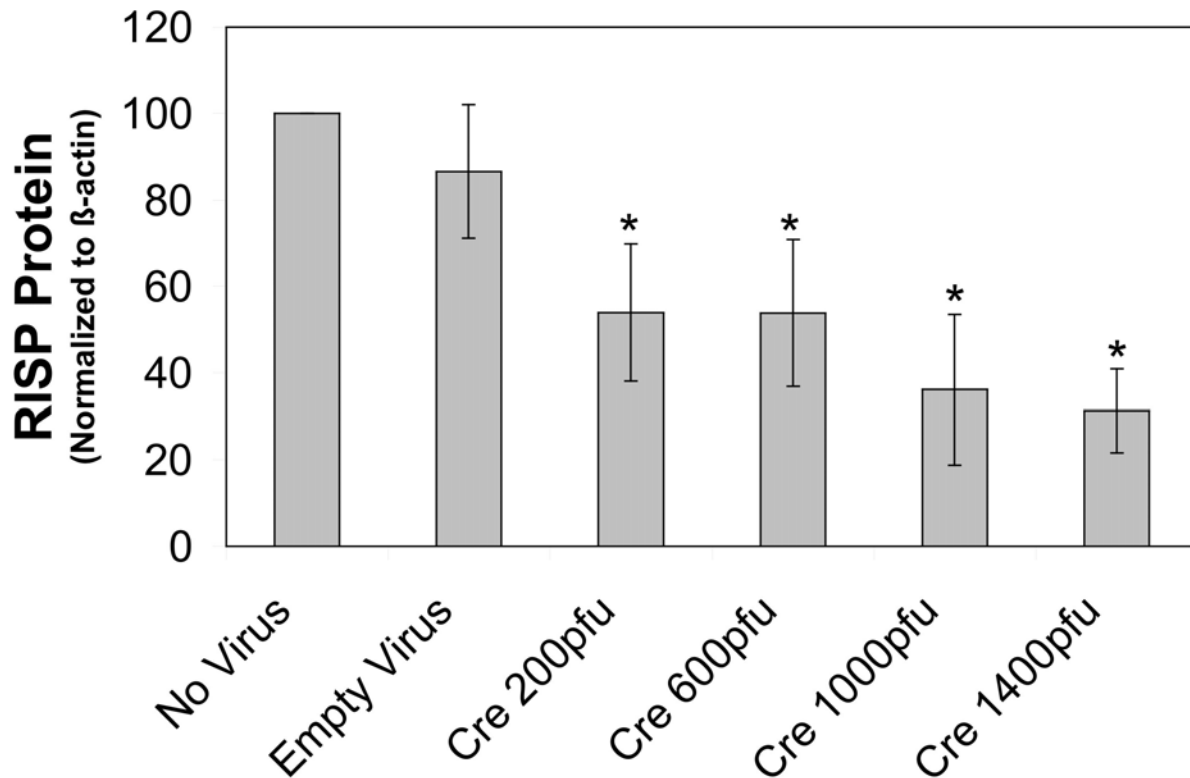
Online Data Supplement Figure 8E (B)

Online Data Supplement Figure 8E (B). Effect of decreased RISP expression on the ability of lung slices to increase cytosolic calcium, as assessed by Fura 2, in response to a receptor-mediated trigger of calcium. Lung slices from Untreated Mice as well as Vehicle-treated mice and Tamoxifen-treated mice were perfused under baseline conditions and then the media was switched to one containing ET-1 (10 nM). The average ET-1-induced change in the Fura 2 ratio was similar across the groups, indicating that decreased RISP expression had no effect on a receptor-mediated increase in cytosolic calcium. Values are means \pm SEM, n=6 lung slices per group.



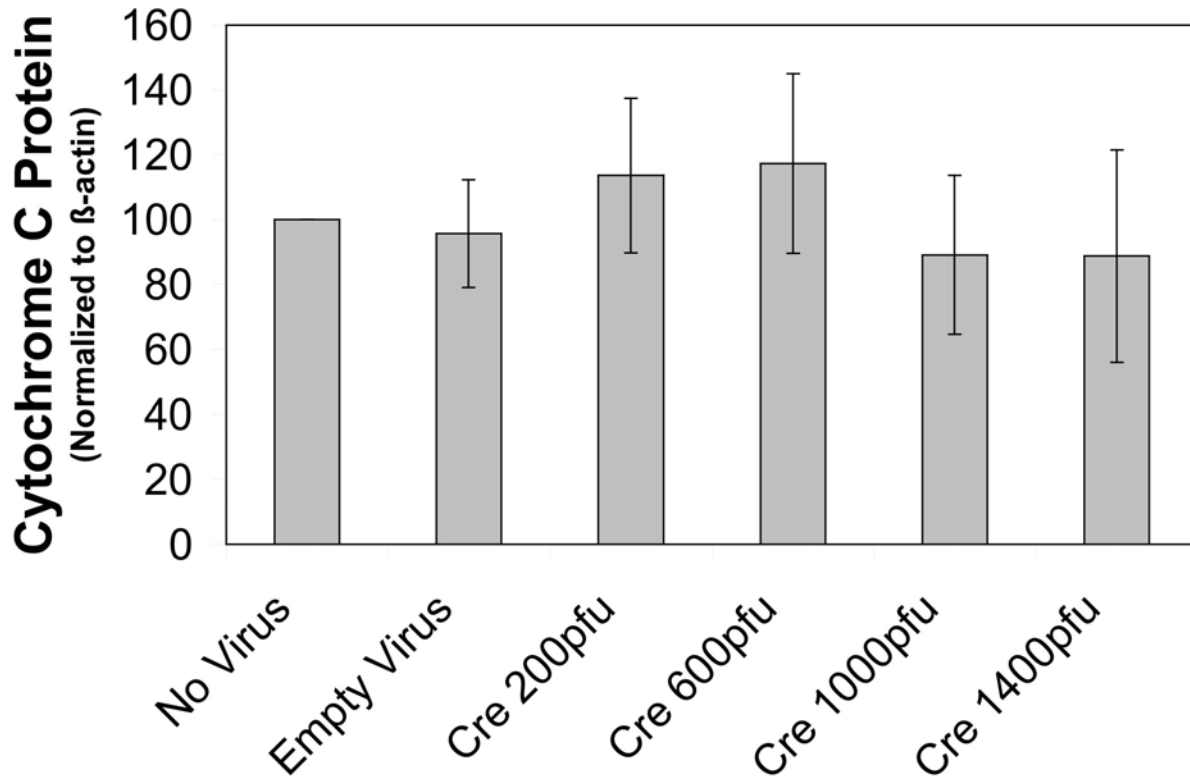
Online Data Supplement Figure 9E A

Online Data Supplement Figure 9E (A). Effect of Cre expression on RISP, cytochrome c, and COX IV expression in PSMC from conditional knockout mice. Western blot of lysates from untransfected (no virus), empty adenovirus transfected (1400 pfu/cell), and Cre-expressing adenovirus-transfected (200, 600, 1000, and 1400 pfu/cell) PSMC from conditional knockout mice probed with antibodies against the RISP subunit, cytochrome c, COX IV or β -actin.



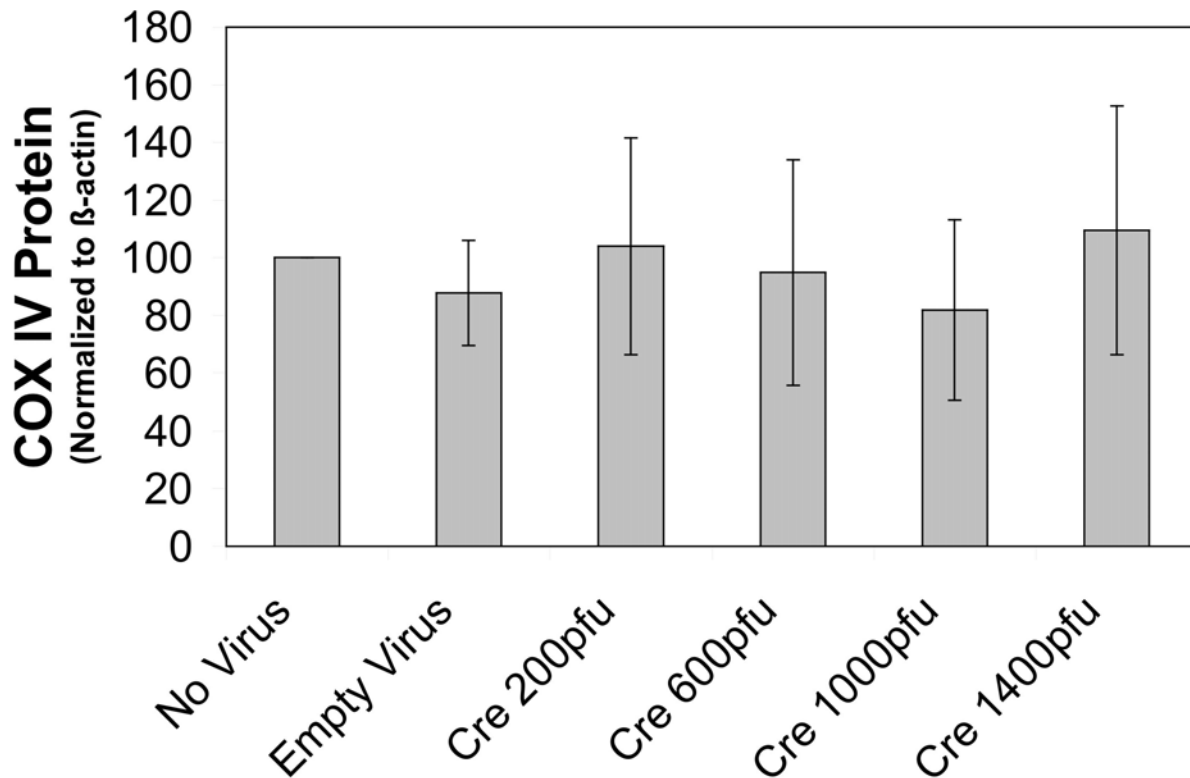
Online Data Supplement Figure 9E B

Online Data Supplement Figure 9E (B). Effect of Cre expression on RISP, cytochrome c, and COX IV expression in PASMC from conditional knockout mice. Quantified analysis of Western blots from untransfected (no virus), empty adenovirus-transfected (1400 pfu/cell), and Cre-expressing adenovirus transfected (200, 600, 1000, and 1400 pfu/cell) PASMC isolated from conditional knockout mice with RISP expression normalized to β -actin. Values are means \pm SEM, n=5 Westerns Blots. *p<0.05 compared to no virus.



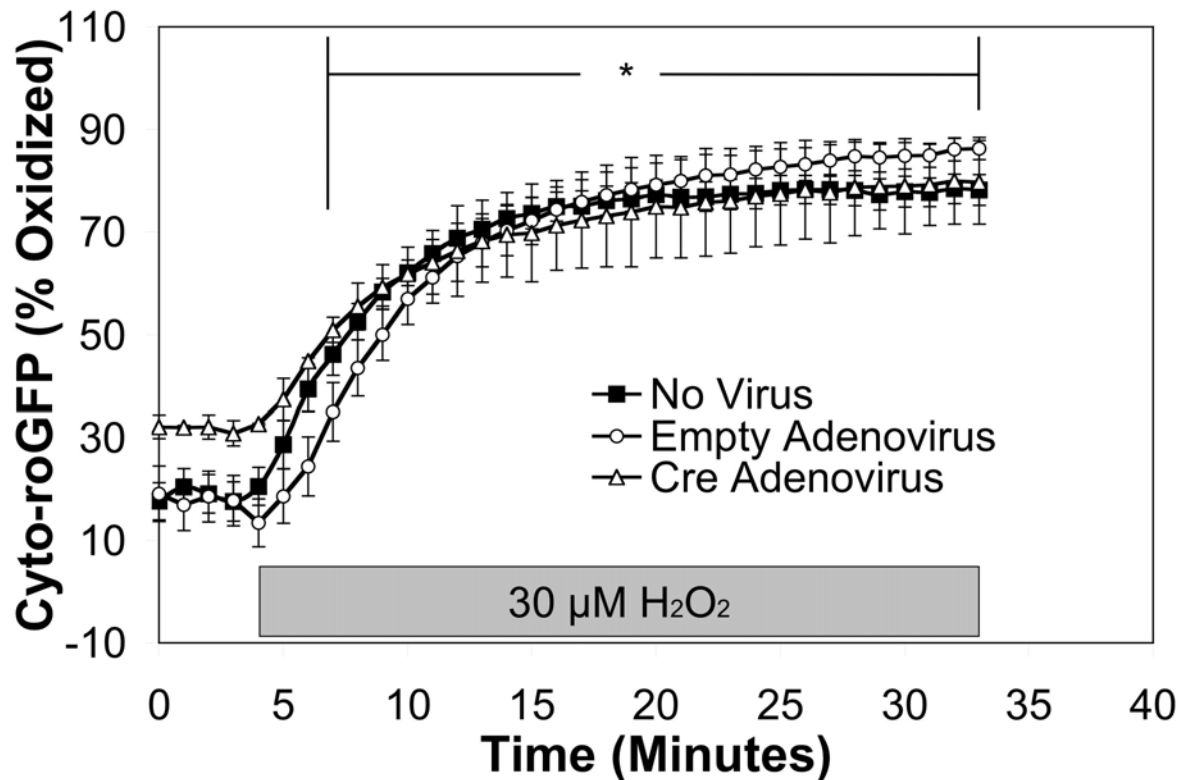
Online Data Supplement Figure 9E C

Online Data Supplement Figure 9E (C). Effect of Cre expression on RISP, cytochrome c, and COX IV expression in PASMIC from conditional knockout mice. Quantified analysis of Western blots from untransfected (no virus), empty adenovirus-transfected (1400 pfu/cell), and Cre-expressing adenovirus-transfected (200, 600, 1000, and 1400 pfu/cell) PASMIC from conditional knockout mice with cytochrome c expression normalized to β -actin. Values are means \pm SEM, n=5 Westerns Blots.



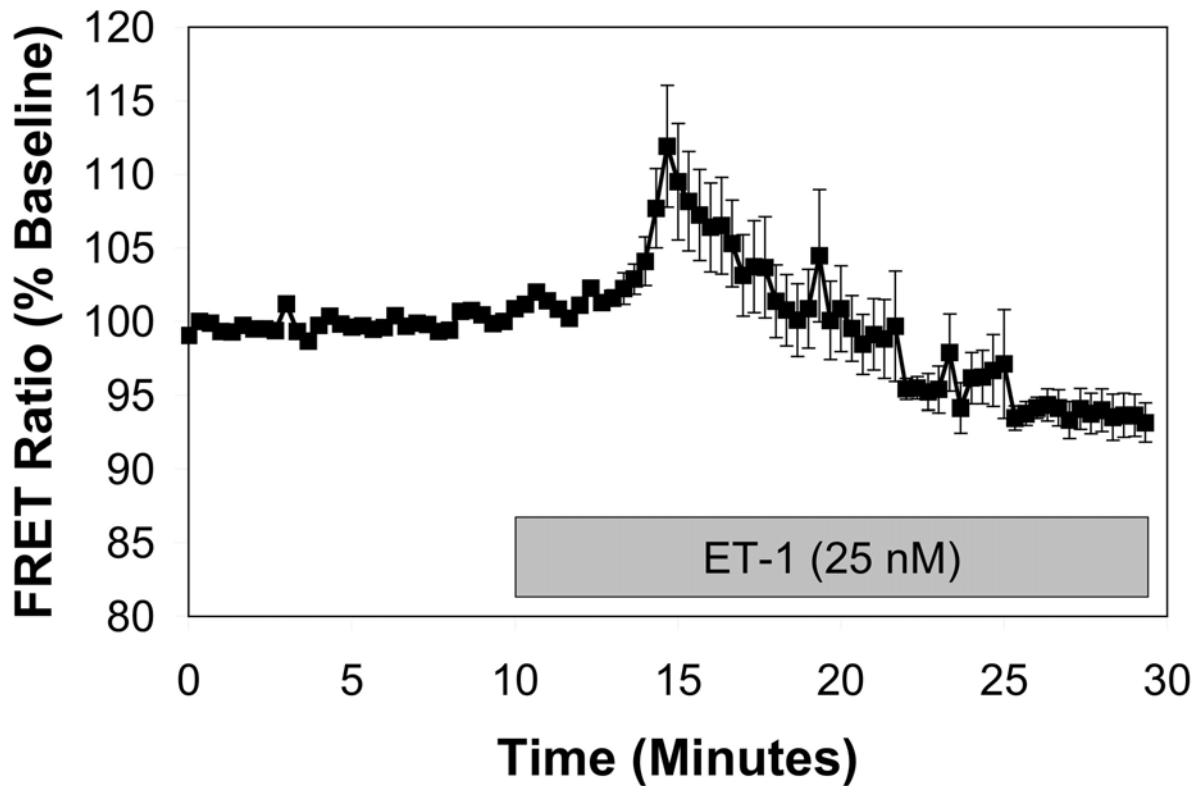
Online Data Supplement Figure 9E D

Online Data Supplement Figure 9E (D). Effect of Cre expression on RISP, cytochrome c, and COX IV expression in PASMIC from conditional knockout mice. Quantified analysis of Western blots from untransfected (no virus), empty adenovirus-transfected (1400 pfu/cell), and Cre-expressing adenovirus-transfected (200, 600, 1000, and 1400 pfu/cell) PASMIC from conditional knockout mice with COX IV expression normalized to β -actin. Values are means \pm SEM, n=5 Westerns Blots.



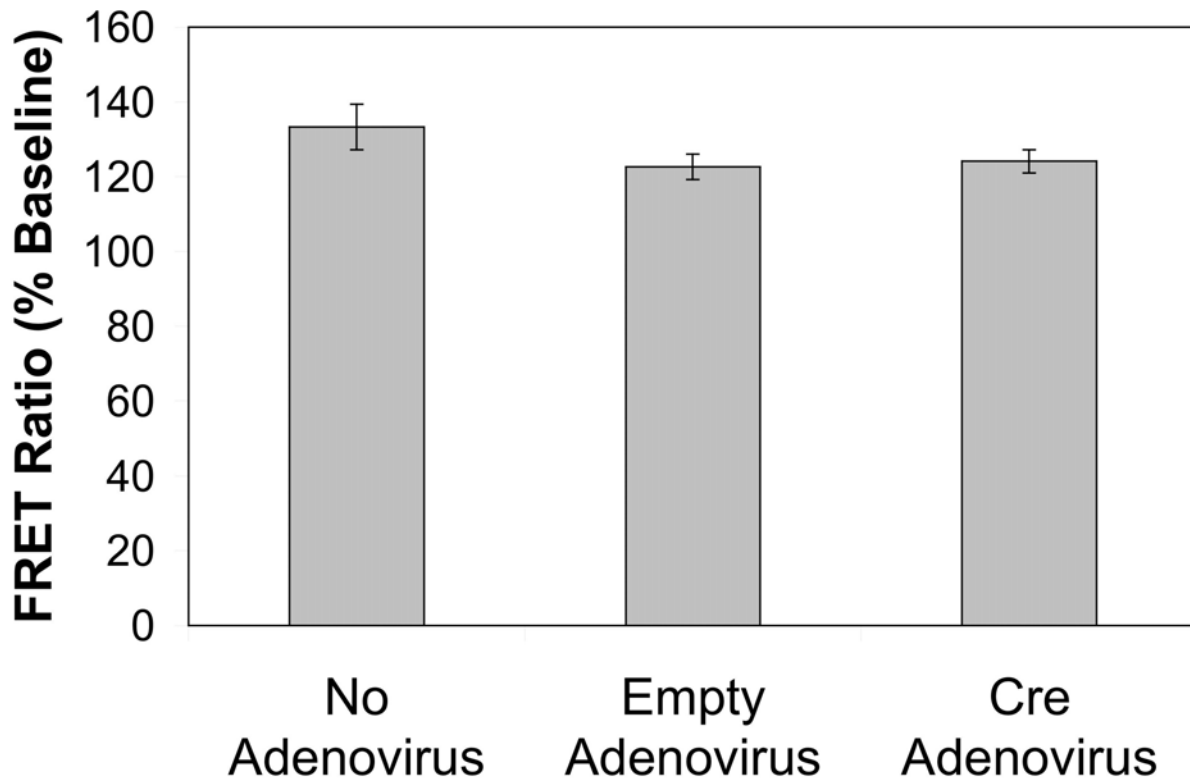
Online Data Supplement Figure 10E

Online Data Supplement Figure 10E. Decreased RISP expression does not affect the ability of Cyto-roGFP to respond to the administration of exogenous hydrogen peroxide. In order to determine whether a decrease in RISP expression could maximally oxidize the Cyto-roGFP under normoxic conditions, control (No Virus), Empty Adenovirus and Cre Adenovirus-transfected PASMIC were perfused under normoxic baseline conditions and then switched to media containing H₂O₂ (30 μM). H₂O₂ significantly increased oxidation of Cyto-roGFP to a similar extent in all groups. This indicates that decreased RISP expression in the Cre Adenovirus-transfected PASMIC does not cause maximal oxidation of Cyto-roGFP and therefore mask the hypoxic response. Values are means ± SEM, n=4 cover slips per experiment. *p<0.05 compared to Baseline.



Online Data Supplement Figure 11E (A)

Online Data Supplement Figure 11E. Effect of decreased RISP expression on the ability of lung slices to increase cytosolic calcium, as assessed by YC2.3 FRET, in response to a receptor-mediated trigger of calcium. PASMCM from a RISP^{flx/flx} mouse were treated with no virus (No Adenovirus), Empty Adenovirus, or Cre Adenovirus. (A) Typical tracing of Empty Adenovirus-transfected PASMCM that were perfused under baseline conditions and then switched to media containing ET-1 (25 nM).



Online Data Supplement Figure 11E (B)

Online Data Supplement Figure 11E. Effect of decreased RISP expression on the ability of lung slices to increase cytosolic calcium, as assessed by YC2.3 FRET, in response to a receptor-mediated trigger of calcium. PASMCM from a RISP^{flox/flox} mouse were treated with no virus (No Adenovirus), Empty Adenovirus, or Cre Adenovirus. The average ET-1 (25 nM)-induced change in the YC2.3 FRET ratio was similar across the groups (B) indicating that adenoviral-treatment of PASMCM had no effect on a receptor-mediated increase in cytosolic calcium. Values are means \pm SEM, n=4 cover slips with 2-3 PASMCM per cover slip.

References

- 1E. Waypa GB, Chandel NS, Schumacker PT. Model for hypoxic pulmonary vasoconstriction involving mitochondrial oxygen sensing. *Circ Res* 2001;88:1259-1266.
- 2E. Waypa GB, Marks JD, Guzy R, Mungai PT, Schriewer J, Dokic D, Schumacker PT. Hypoxia triggers subcellular compartmental redox signaling in vascular smooth muscle cells. *Circ Res* 2010;106:526-535.
- 3E. Wirth A, Benyo Z, Lukasova M, Leutgeb B, Wettschureck N, Gorbey S, Orsy P, Horvath B, Maser-Gluth C, Greiner E, et al. G12-g13-larg-mediated signaling in vascular smooth muscle is required for salt-induced hypertension. *Nat Med* 2008;14:64-68.
- 4E. Dooley CT, Dore TM, Hanson GT, Jackson WC, Remington SJ, Tsien RY. Imaging dynamic redox changes in mammalian cells with green fluorescent protein indicators. *J Biol Chem* 2004;279:22284-22293.
- 5E. Hanson GT, Aggeler R, Oglesbee D, Cannon M, Capaldi RA, Tsien RY, Remington SJ. Investigating mitochondrial redox potential with redox-sensitive green fluorescent protein indicators. *J Biol Chem* 2004;279:13044-13053.
- 6E. Cannon MB, Remington JS. Redox-sensitive green fluorescent protein: Probes for dynamic intracellular redox responses. A review. *Methods Mol Biol* 2009;476:50-64.
- 7E. Lohman JR, Remington SJ. Development of a family of redox-sensitive green fluorescent protein indicators for use in relatively oxidizing subcellular environments. *Biochemistry* 2008;47:8678-8688.
- 8E. Jiang K, Schwarzer C, Lally E, Zhang S, Ruzin S, Machen T, Remington SJ, Feldman L. Expression and characterization of a redox-sensing green fluorescent protein (reduction-oxidation-sensitive green fluorescent protein) in arabidopsis. *Plant Physiol* 2006;141:397-403.

- 9E. Waypa GB, Guzy R, Mungai PT, Mack MM, Marks JD, Roe MW, Schumacker PT. Increases in mitochondrial reactive oxygen species trigger hypoxia-induced calcium responses in pulmonary artery smooth muscle cells. *Circ Res* 2006;99:970-978.
- 10E. Miyawaki A, Llopis J, Heim R, McCaffery JM, Adams JA, Ikura M, Tsien RY. Fluorescent indicators for Ca^{2+} based on green fluorescent proteins and calmodulin. *Nature* 1997;388:882-887.
- 11E. Miyawaki A, Griesbeck O, Heim R, Tsien RY. Dynamic and quantitative Ca^{2+} measurements using improved cameleons. *Proc Natl Acad Sci U S A* 1999;96:2135-2140.
- 12E. Griesbeck O, Baird GS, Campbell RE, Zacharias DA, Tsien RY. Reducing the environmental sensitivity of yellow fluorescent protein. Mechanism and applications. *J Biol Chem* 2001;276:29188-29194.
- 13E. Desireddi JR, Farrow KN, Marks JD, Waypa GB, Schumacker PT. Hypoxia increases ROS signaling and cytosolic Ca^{2+} in pulmonary artery smooth muscle cells of mouse lungs slices. *Antioxid Redox Signal* 2010;12:595-602.
- 14E. Wallenstein S, Zucker CL, Fleiss JL. Some statistical methods useful in circulation research. *Circ Res* 1980;47:1-9.